2019-11-22

Advanced Electromyogram Signal Processing with an Emphasis on Simplified, Near-Optimal Whitening

He Wang
Worcester Polytechnic Institute

Advanced Electromyogram Signal Processing with an Emphasis on Simplified, Near-Optimal Whitening

by

He Wang

A Thesis

Submitted to the Faculty

of the

WORCESTER POLYTECHNIC INSTITUTE

in partial fulfillment of the requirements for the

Degree of Master of Science

in

Electrical and Computer Engineering

November 2019

APPROVED:

_____

Dr. Edward A. Clancy, Research Advisor

_____

Dr. Xinming Huang, Committee Member

_____

Prof. Stephen J. Bitar

ABSTRACT

Estimates of the time-varying standard deviation of the surface EMG signal (EMGσ) are extensively used in the field of EMG-torque estimation. The use of a whitening filter can substantially improve the accuracy of EMGσ estimation by removing the signal correlation and increasing the statistical bandwidth. However, a subject-specific whitening filter which is calibrated to each subject, is quite complex and inconvenient. To solve this problem, we first calibrated a 60th-order "Universal" FIR whitening filter by using the ensemble mean of the inverse of the square root of the power spectral density (PSD) of the noise-free EMG signal. Pre-existing data from elbow contraction of 64 subjects, providing 512 recording trials were used. The test error on an EMG-torque task based on the "Universal" FIR whitening filter had a mean error of 4.80% maximum voluntary contraction (MVC) with a standard deviation of 2.03% MVC. Meanwhile the subject-specific whitening filter had performance of 4.84±1.98% MVC (both have a whitening band limit at 600 Hz). These two methods had no statistical difference.

Furthermore, a 2nd-order IIR whitening filter was designed based on the magnitude response of the "Universal" FIR whitening filter, via the differential evolution algorithm. The performance of this IIR whitening filter was very similar to the FIR filter, with a performance of 4.81±2.12% MVC. A statistical test showed that these two methods had no significant difference either.

Additionally, a complete theory of EMG in additive measured noise contraction modeling is described. Results show that subtracting the variance of whitened noise by computing the root difference of the square (RDS) is the correct way to remove noise from the EMG signal.

ACKNOWLEDGEMENT

Foremost, I am sincerely thankful to my research advisor Professor Edward A. Clancy. Professor Clancy is the one who lead me to the biomedical engineering field and keep giving me precious advice. I really appreciate his guidance, not only for my research and projects, but also letting me know how much I can do to contribute to this world as an electrical engineer. I am excited about continuing my Ph.D. with him in the future.

I also want to thank my senior colleagues Ziling Zhu and Jiannan Li. They gave me a lot of valuable advice during the research. Also, Dr. Chenyun Dai's previous studies make all my research possible, appreciate his excellent work.

My teammates Haopeng Wang and Kiriaki J. Rajotte are brilliant students and most helpful colleagues. Although we worked on different aspects in this project, I couldn't overcome obstacles without their help and advice.

Last but not the least, no word can express my appreciation to my parents who always support me unconditionally. The family's love encourages me moving forward bravely. Thank you all!

CONTRIBUTIONS

This whole project is a team project. Kiriaki J. Rajotte and Haopeng Wang also provided their best work to complete this project. All the data were collected during previous experiments. To test our new technique, we used Chenyun Dai's method as our baseline. What's more, we tested our new technique by using Dr. Clancy's EMG signal processing toolbox. There are three basic parts for our project, "Universal" whitening filter, new features test and noise cancellation. I mainly focused on calibrating the "Universal" FIR and IIR whitening filters and testing the performance of them; Kiriaki J. Rajotte focused on combining the new features and testing the performance; Haopeng Wang focused on the noise cancellation and modeling. In fact, most of the work was finished together by all of us under the guidance of Prof. Clancy. This project couldn't be done without our teamwork.

Content

CHAPTER 1 – INTRODUCTION AND BACKGROUND

For this part, a contribution part will briefly introduce the whole teamwork research project and my work in this project. The background and goal of this thesis is introduced. Also, some biomedical knowledge related to this thesis is mentioned, some signal processing techniques is introduced. The method for data collection is shown. And then, the final section summarizes my MS work and briefly introduce the main content of following chapters.

I. EMG BASICS

Structure of Muscle and Motor Unit

There are two basic kinds of human muscle fibers, slow twitch fibers (Type 1) and fast twitch fibers (Type 2). Slow twitch fibers can generate low level force for a long period without fatigue; fast twitch fibers are capable of generating quicker, more powerful contraction, but this kind of contraction cannot last a long period and people can easily fatigue. Different kinds of movements can be achieved by using these two kinds of muscle fibers together. Figure 1 shows the structure of skeletal muscle. The muscle structure always includes parallel muscle fascicles. These fascicles are a collection of parallel muscle fibers which are innervated by attached neurons. Figure 2 shows the structure of one muscle unit which is formed by one motor nerve and all innervated muscle fibers. All muscle fibers in the same motor unit have the same type. When contraction happens, all innervated muscle fibers in one motor unit subsequently contract, this is called “all or nothing” rule. A group of motor units build up one muscle, these motor units work together to coordinate different kinds of contractions.

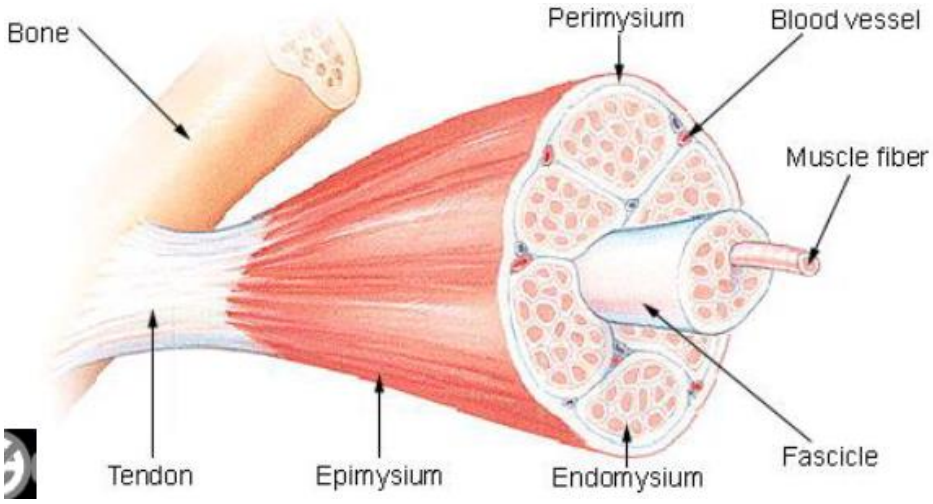

Fig. 1: The structure of skeletal muscle [1]

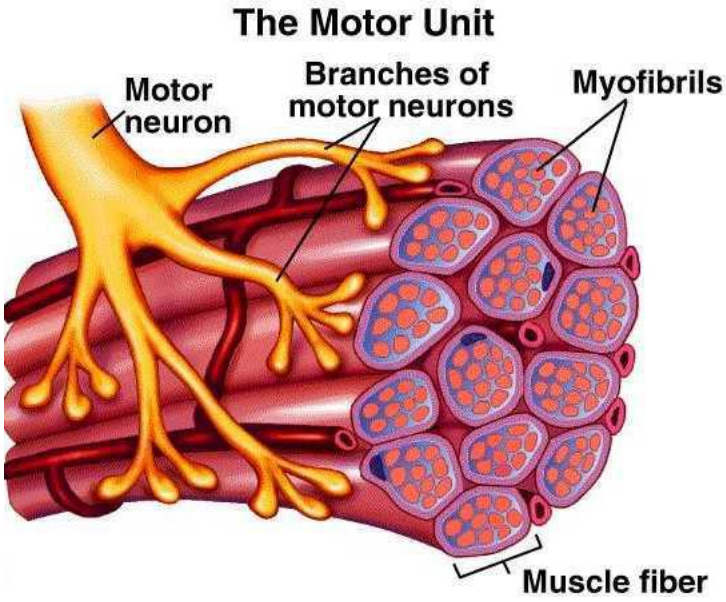

Fig. 2: The structure of muscle unit [2]

Muscle Electrical Activity and Its Engineering Model

Muscle fibers are electro-chemically activated by motor neurons when the central nerve system sends commands to motor neurons. Fibers will depolarize once they are activated, and the fibers will repolarize to a rest state after depolarization. This whole electrical process generates an electromagnetic field.

The electromagnetic field can be recorded within muscle (indwelling EMG) or on the skin surface (surface EMG). Indwelling EMG requires electrical needles/wires penetrating human skin; surface EMG is a non-invasive method to collect EMG signals.

Figure 3 shows the whole process of depolarization-repolarization in one motor unit. When muscle fibers are at rest state, the rest potential is around –70 mV, which is based on the concentration of ions in body cells and fluid. When muscle fibers are activated and depolarize, the action potential peaks go up to around +30 mV. The duration of one action potential is usually 2 –4 ms or longer. Different motor units usually have different potential shapes with different action potentials. Different number of motor units are required when different movements are performed. Firing rate is the frequency of motor unit to discharge. When a motion with more force is performed, more activated motor units are required, and the firing rate of each motor unit will increase. The process of activating more motor units is called the recruitment of motor units. The force level is measured by percent maximum voluntary contraction (%MVC) level. Usually, the firing rate is about 5 –10 pulses per second when initially recruited and can be up to 20+ pulses per second at the highest force levels

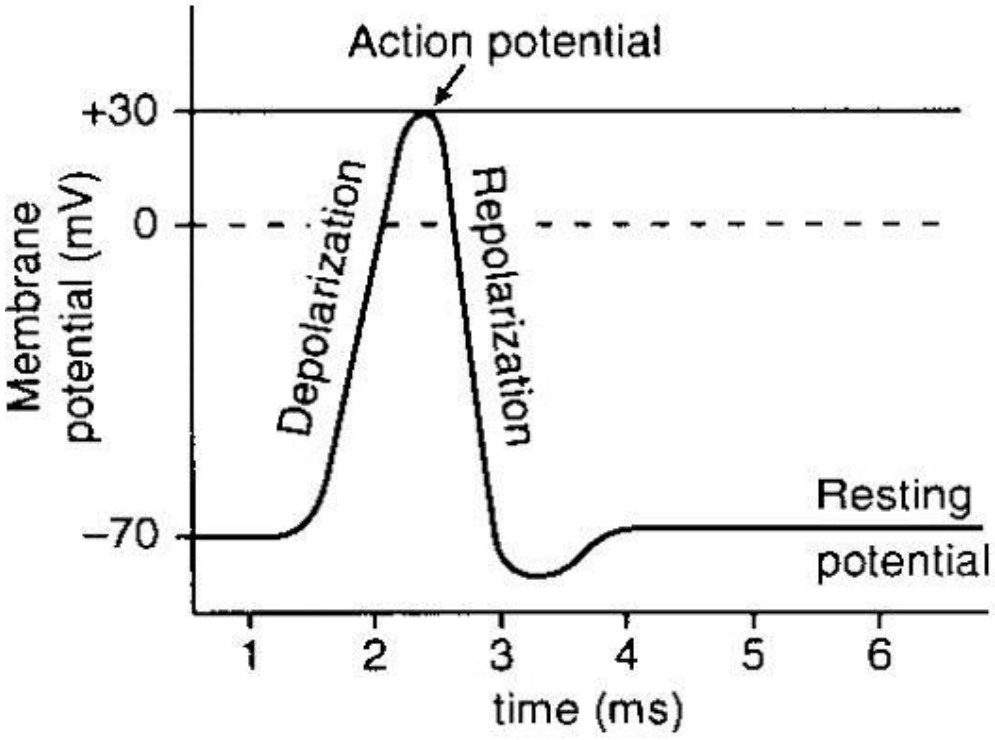

Fig. 3: Electrical activity of a motor unit [3]

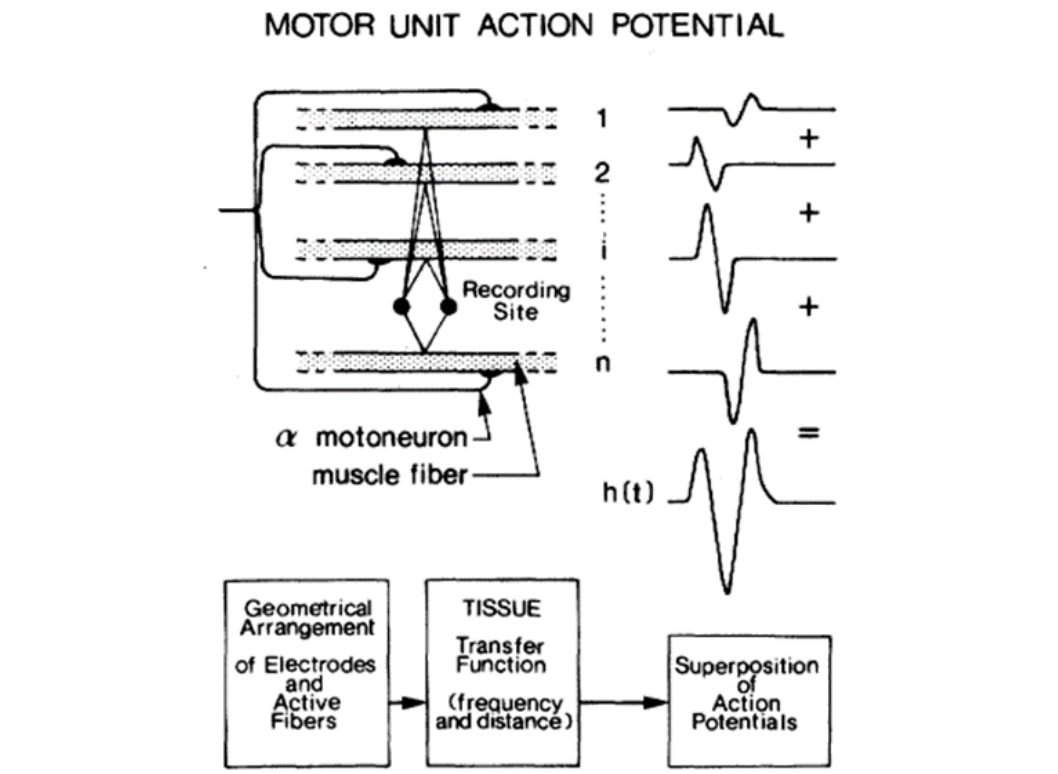

Fig. 4: Schematic representation of the generation of the motor unit action potential [4]

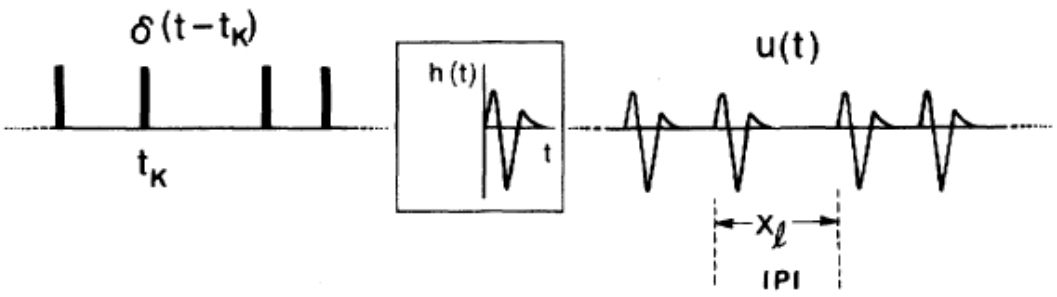

Fig. 5: Schematic for the motor unit action potential train [4]

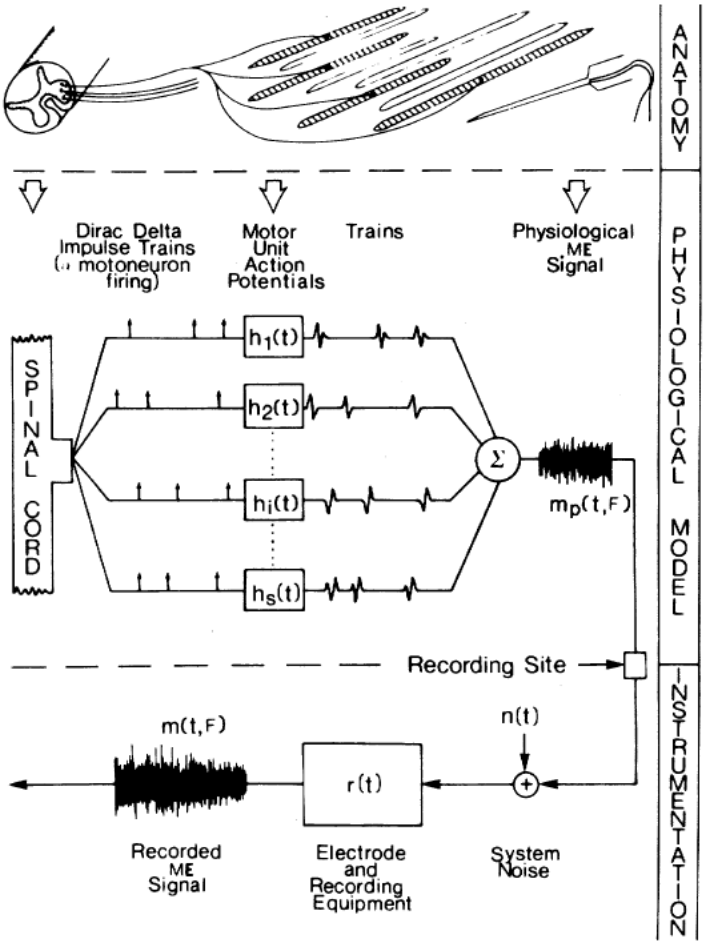

Fig. 6: Complete engineering model of motor unit action potential [4]

Figure 5 shows that one motor unit always generates a very similar shape; this shape may vary because of muscle fatigue or disease. For different contraction force levels, different number of motor units will discharge and activate at the same time. Figure 4 shows this case as the superposition of potentials from individual fibers.

Nerve commands a series of stimuli which can be treated as an impulse train to the innervated muscle fibers, the output can be treated as an impulse response train. The EMG recording is the summation of all the impulse response trains when motor units discharge at the same time. So, the EMG recording looks like a random Gaussian process. Figure 6 shows the total engineering model.

Basic EMG Signal Processing Methods

Raw EMG signal contains lots of noise and interference. As mention before, the EMG signal is the summation of multiple impulse response trains and can be regarded as an

amplitude modulated, zero-mean, random Gaussian process

$$m[n] = s[n] \cdot v[n] \qquad (1),$$

where n is the discrete time sample index, $m[n]$ is raw EMG signal, $s[n]$ is the EMG standard deviation (EMGσ) and $v[n]$ is a random process with unit variance. EMGσ is the useful information which can be used to estimate force. Studies have been developed to improve the estimation of EMGσ [6, 7 , 8, 9] Figure 7 shows EMGσ from raw EMG signal.

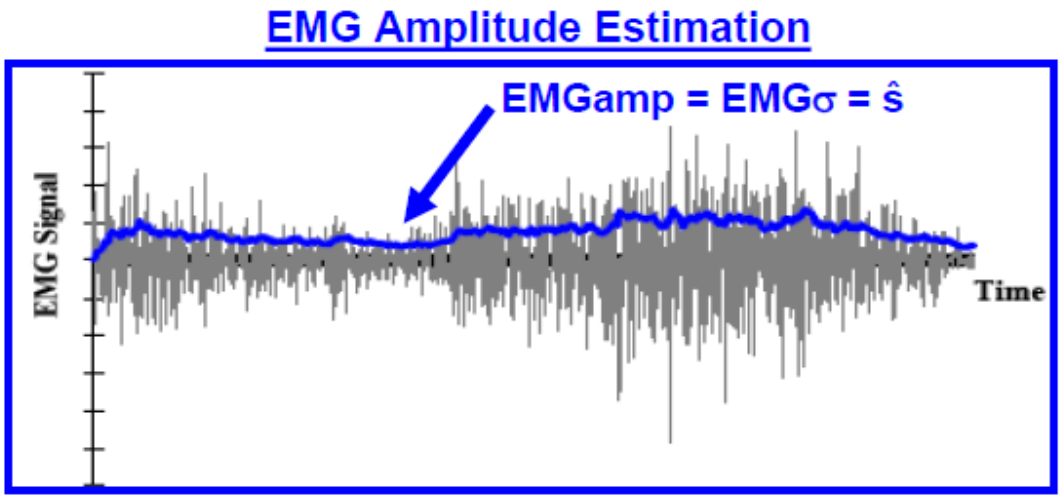

Fig. 7: Diagram of EMG amplitude estimation [5]

There are two basic EMG estimators: moving average root mean square (MARMS) processor and moving average mean absolute value (MAMAV) processor,

MARMS processor:

$$\hat{s}_{RMS} = \sqrt{\frac{1}{L} \cdot \sum_{k=n-L+1}^{n} m^2[k]} \qquad (2)$$

MAMAV processor:

$$\hat{s}_{MAV} = \frac{1}{L} \cdot \sum_{k=n-L+1}^{n} |m[k]| \qquad (3)$$

where L is the window length.

These two estimators can be thought of as the cascade of a non-linear detector, a smoother (low-pass filter) and a linearizer (return signal to proper units). Figure 8 shows this cascade.

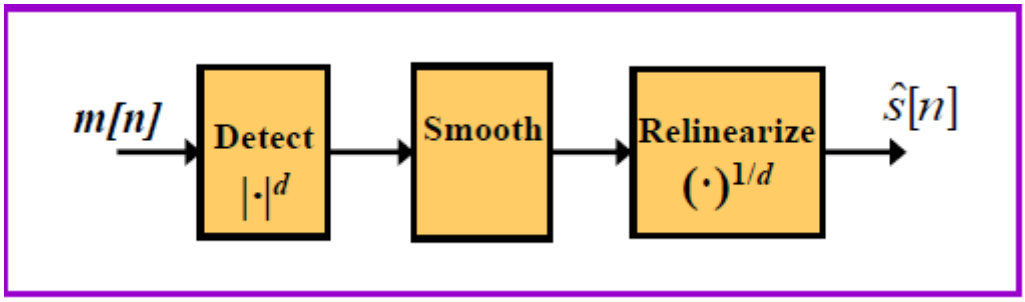

Fig. 8: EMG estimator cascade

The detector and linearizer can be replaced by a rectifier if $d = 1$.

For a single site EMG signal, there are several techniques that can help improve the estimation of EMGσ [6, 7]. A 2nd-order notch filter at 60 Hz and its harmonics is applied to remove the powerline interference. A 4th-order highpass filter with cutoff frequency at 15 Hz is applied prior to RMS or MAV estimator to attenuate motion artifact; a higher cutoff frequency may lead to loss of EMG signal. Since EMG signal is highly correlated, a whitening filter is applied to remove the correlation and increase the statistical bandwidth. The original subject-specific whitening filter includes two stages [6] : a fixed whitening shape and an adaptive noise canceler. This thesis will mainly focus on improving and simplifying this original whitening filter to make it easier to implement. Figure 9 shows the complete process of single site EMG processing.

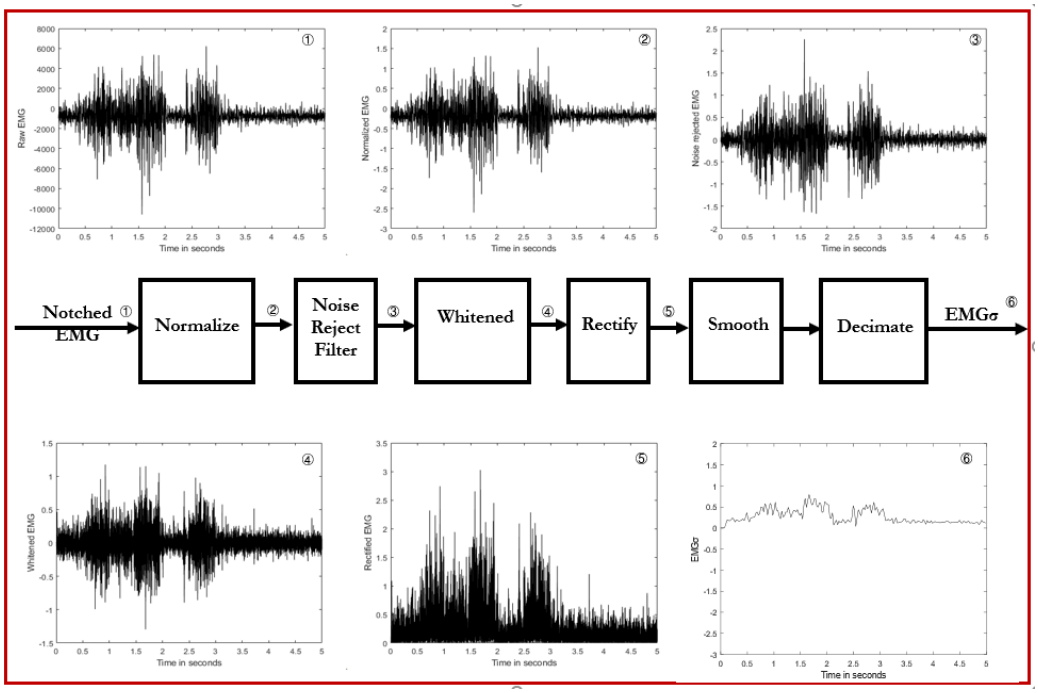

Fig. 9: Single site EMG signal processing

Studies on multiple channel EMG signal [5, 10, 11, 12] show that by combining EMG signal recorded by different electrodes placed adjacent to each other, the performance of EMGσ estimation can be significantly improved. A normalization process is needed to eliminate the gain difference between channels. Figure 10 shows the complete process of multi-channel EMG processing.

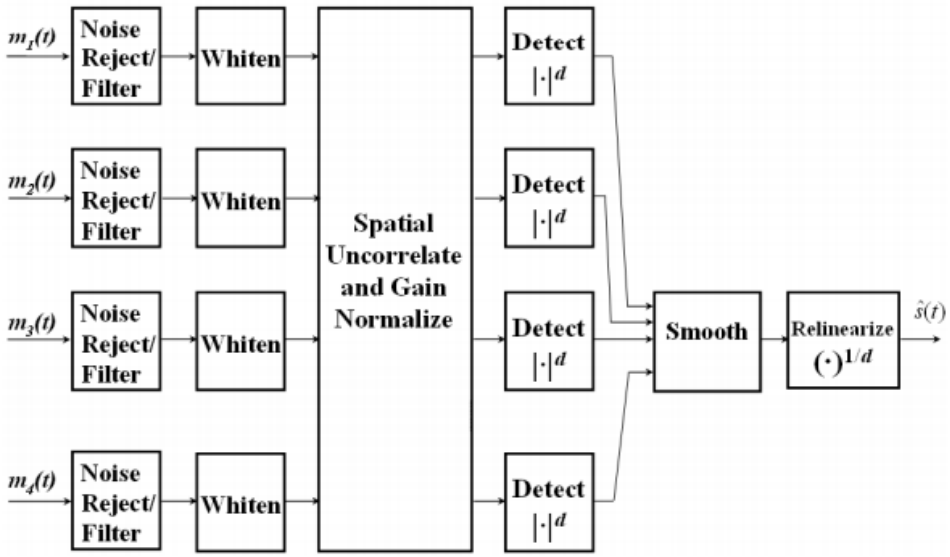

Fig. 10: Six stages multi-channel EMG processor [8]

II. INTRODUCTION OF REMAINING CHAPTERS

The remaining chapters will include all of my MS work in detail in the form of published, submitted journal or conference manuscripts and also description of work that is not mentioned in the manuscripts which will be presented in a traditional thesis formation.

Chapters 2 and 3 introduce "Universal" whitening filter. In Chapter 2, the "Universal" FIR whitening filter is briefly introduced. This chapter was published as a conference paper. Chapter 3 describes the "Universal" IIR filter. This chapter is presented in traditional thesis formation. A differential evolution method will be introduced to calibrate this IIR whitening filter.

Chapter 4 and appendix I is about EMG noise signal modeling and root difference of squares (RDS) computation to subtract noise. Chapter 4 was submitted as a journal

paper. Appendix I shows the details that are not covered in Chapter 4 including some results and analysis.

Appendix II shows the detail of data used in this thesis including all the subject numbers, trial numbers, replaced trial numbers and substituted trial numbers.

REFERENCES FOR THIS CHAPTER

[1] http://en.wikipedia.org/wiki/Muscle_fascicle.

[2] http://academic.wsc.edu/faculty/jatodd1/351/ch6outline.html.

[3] http://www.physicsforums.com/showthread.php?t=473984.

[4] DeLuca**,** "Physiology and mathematics of myoelectric signals," *IEEE Trans Biomed Eng* 26(6): 313–325, 1979.

[5] Edward A. Clancy, Stochastic Modeling of the Relationship Between the Surface Electromyogram and Muscle Torque. Ph.D. Thesis, Massachusetts Institute of Technology, January 1991.

[6] Edward A. Clancy and Kristin A. Farry, "Adaptive Whitening of the Electromyogram to Improve Amplitude Estimation," IEEE Transactions on Biomedical Engineering, Vol. 47, No. 6, pp. 709-719, 2000.

[7] Edward A. Clancy and Neville Hogan, "Multiple Site Electromyograph Amplitude Estimation," IEEE Transactions on Biomedical Engineering, Vol. 42, No. 2, pp. 203-211, 1995.

[8] Edward A. Clancy, Stéphane Bouchard and Denis Rancourt, "Estimation and Application of Electromyogram (EMG) Amplitude During Dynamic Contractions," IEEE Engineering in Medicine and Biology Magazine, Vol. 20, No. 6, pp. 47-54, 2001.

[9] Potvin, J.R., and Brown, S. 2004. Less is more: high-pass filtering, to remove up to 99% of the surface EMG signal power, improves EMG-based biceps brachii muscle force estimates. J. Electromyogr. Kinesiol. 14: 389–399. doi:10.1016/j.jelekin. 2003.10.005. PMID:15094152.

[10] Hogan, N. and R. W. Mann, "Myoelectric signal processing: Optimal estimation applied to electromyography-Part II: Experimental demonstration of optimal myoprocessor performance," IEEE Trans. Biomed. Eng., vol. BME-27, pp. 396-410, 1980b.

[11] Harba, M. I. A. and P. A. Lynn, "Optimizing the acquisition and processing of surface electromyographic signals," J. Biomed. Eng., vol. 3, pp. 100-106, 1981.

[12] Hogan, N. and R. W. Mann, "Myoelectric signal processing: Optimal estimation applied to electromyography-Part I: Derivation of the optimal myoprocessor," IEEE Trans. Biomed. Eng., vol. BME-27, pp. 382-395, 1980a.

CHAPTER 2 – SIMPLIFIED IMPLEMENTATION OF OPTIMIZED WHITENING OF THE ELECTROMYOGRAM SIGNAL

This chapter has been published in 2019 *Northeast Bioengineering Conference* as He Wang, Kiriaki J. Rajotte, Haopeng Wang, Chenyun Dai, Ziling Zhu, Moinuddin Bhuiyan, Edward A. Clancy, "*Simplified Implementation of Optimized Whitening of the Electromyogram Signal*."

Introduction: The surface electromyogram (EMG) signal is well modeled as an amplitude modulated, correlated random process. The amplitude modulation, defined as the time-varying standard deviation (EMGσ) of the signal, is used in various applications as a measure of muscle effort, e.g., EMG-force models, prosthesis control, clinical biomechanics and ergonomics assessment. EMGσ can be estimated by rectifying the EMG and then lowpass filtering (cutoff ~1 Hz). However, it has long been known that the correlated nature of EMG reduces the statistical efficiency of the EMGσ estimate, producing a large variance.

To combat this problem, a whitening filter can be used prior to the rectifier. Whitening removes signal correlation—while preserving signal standard deviation—producing a substantially improved EMGσ. The advantages of whitening filters have been known since at least 1974 [3]—yet, few researchers use them. A key limitation to widespread use is that most whiteners are "calibrated" to each subject, making them cumbersome to implement.

Since EMG whitening filters have low gain at low frequencies and higher gain at high frequencies, Potvin [4] implemented simple whitening via a fixed, low-order, FIR, highpass filter that was not calibrated to individual subjects. This approach was not compared to the established technique of subject-specific whitening filters.

Our work reported herein describes development of a simplified whitening technique that relies only on EMG magnitude normalization (a measure that is already common). We compare this technique to state-of the art subject-specific whitening.

Experimental Methods: Pre-existing data from 64 subjects [5] were used and did not require human studies supervision per the WPI IRB. Four electrodes over the biceps and four over the triceps muscles were acquired during three trials of 30-s duration, constant-posture, force-varying elbow contractions in which subjects followed a target displaying a 1 Hz bandlimited, uniform and random process, spanning 50% maximum voluntary contraction (MVC) flexion to 50% MVC extension. Using our existing subject-specific technique to form whitening filters for each electrode (calibrated from additional 5-s rest recordings and constant-effort 50% MVC trials, and limited to 600 Hz in frequency [6,7]), we related EMGσ to force. This EMGσ-force model used each of the eight EMGσ values as inputs, a 15th-order dynamic FIR model per EMGσ, additionally included the squared value of each EMGσ at the 15 time lags (to model the EMG-force non-linearity), and was trained from two trials using least squares. The average ± std. dev. test error on the distinct third trials was 4.84±1.98% flexion MVC (%MVCF). This error served as our "baseline" performance.

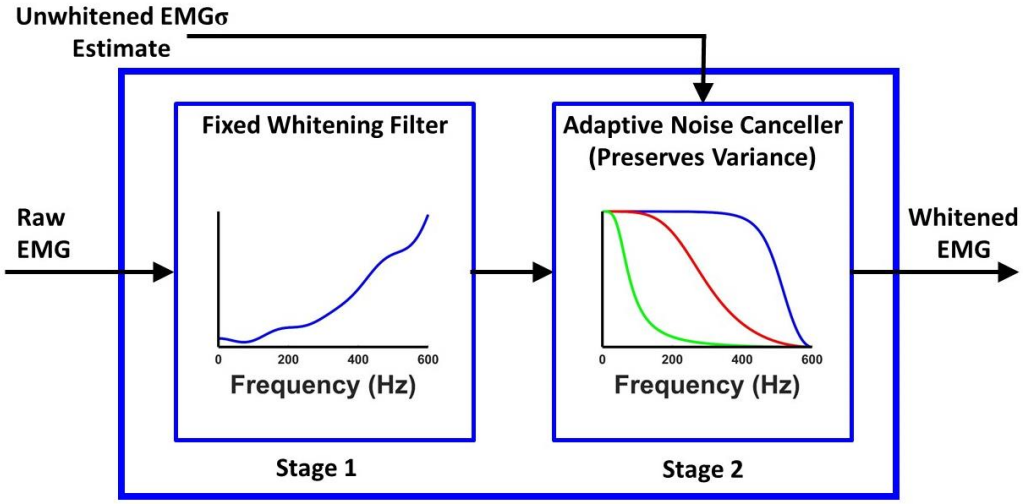

Fig. 1. Two-stage adaptive whitening filter [6].

Analysis Methods and Results: Our whitening filters (Fig. 1) are comprised of a fixed whitening filter followed by an adaptive noise canceller (with variance preservation). The first stage is a fixed linear filter whose magnitude response is the inverse of the square root of the power spectral density (PSD) of the noise-free EMG signal (estimated by subtracting the 0% MVC PSD from the 50% MVC PSD). This filter has low gain at low frequencies and higher gain at high frequencies—the opposite of the spectral

content of EMG. The second stage cancels high frequency noise, above the dominant frequency of EMG. This filter is a time-varying lowpass filter, with a cut-off frequency that is lower at lower effort levels. The time adaptation is set via a first-pass unwhitened EMGσ estimate. The gain of this stage preserves the overall power of the noise-free signal, so that the full whitening process does not alter EMGσ.

We contrasted subject-specific whitening filter calibration to "universal" calibration. Each EMG was gain normalized, to account for gain variations between channels. Thereafter, the 0% MVC PSDs and (separately) the 50% MVC PSDs were ensemble-averaged across the 512 calibration recordings (64 subjects x 8 electrodes/subject). The one, ensemble-averaged 0% MVC and the one, ensemble-averaged 50% MVC were then used to form a single "universal" two-stage whitening filter. This filter was then similarly evaluated on the EMG-force data, producing an average ± std. dev. test error of 4.80±2.03 %MVCF—the same as that of subject-specific whiteners.

Conclusions: Our work, combined that of Potvin [4], suggest that the PSD of EMG is sufficiently consistent subject-to-subject that subject-specific calibration of PSDs for EMG whitening may not be necessary (for noise cancellation). Only a gain normalization may be needed per channel. Note that PSD shapes are known to vary with inter-electrode distance [1] and might vary muscle-to-muscle. Also, this set of dynamic contractions may not be particularly sensitive to the magnitude of the noise power, since few of the active-trial contractions were near 0% MVC. (Noise is most impactful at low contraction levels.)

References:

1. Hogan N et al. IEEE TBME. 1980;27:396–410.
2. Clancy EA et al. IEEE TBME. 1995;42:203–211.
3. Kaiser E et al. In "Control of Upper-Extremity Prosthetics & Ortho.," Charles C. Thomas, 1974:54–57.
4. Potvin et al. J Electromyo Kinesiol. 2004;14:389–399.
5. Dai et al. IEEE TNSRE. 2017;25:1529–1538.
6. Clancy et al. IEEE TBME. 2000;47:709–719.
7. Dasog et al. IEEE TNSRE. 2014;22:664-670.

CHAPTER 3 – STUDY AND IMPLEMENTATION OF "UNIVERSAL" IIR FILTER

I. INTRODUCTION

In Chapter 2, a 60th-order FIR universal whitening filter was introduced. However, from Potvin [1], we know that an IIR highpass filter is enough to take the role of whitening. Such being the case, there will be no need to implement a more complex FIR filter with inefficient coefficients.

Compared to Potvin [1], who had a limited number of subjects, we are provided with a huge number of valuable data, 64 subjects with 512 trials. Since we already calibrated a FIR whitening filter in Chapter 1, we can use the properties of this filter to calibrate an IIR filter.

In this chapter, the method to calibrate an IIR whitening filter will be introduced. To evaluate the performance the IIR whitening filter, we also show the performances of original whitening filter which is calibrated to each subject and FIR whitening filter.

It is hypothesized that by implementing a "Universal" IIR whitening filter which is close enough to the "Universal" FIR whitening filter that has been proven feasible, estimating surface-based EMG to toque will be much more convenient and achievable.

Designing an IIR filter always has some obstacles [2, 3, 4]. The first is that the filter may become unstable; limiting the coefficients can solve this problem. Another problem is that the error surface may have multiple minima [5], thus basic conventional methods can easily get stuck at a local minima and fail to find the global minima. To solve this problem, several algorithms have been introduced such as ant colony optimization (ACO) [6], simulated annealing (SA) [7, 8, 9] and genetic algorithm (GA) [10, 11, 12 ,13, 14, 15]. Among these algorithms, GA is the one applied most when designing an IIR filter.

However, GA is not good at local search ability and the convergence can be premature. Such being the case, a differential evolution (DE) is introduced [16]. Previous work [5] has shown that DE has a better performance than GA when designing an IIR filter.

Hence, DE algorithm was implemented to design the "Universal" IIR whitening filter.

II. METHODS

In this section, methods to calibrate the "Universal" IIR whitening filter will be introduced. Also, methods to evaluate this filter will be shown.

Differential Evolution Algorithm

DE is a global optimization algorithm and stochastic direct search. This algorithm maintains a certain number of population, for each iteration, recombination, evaluation and selection will optimize each candidate of the population. After certain number of iteration or other criteria are met, an optimized solution will be given. For IIR filter design, it is believed that the solution has a global minimum error in the error surface. Basic DE algorithm is shown below.

Initialization
Evaluation
REPEAT
    Mutation
    Crossover
    Evaluation
    Selection
UNTIL (Criteria are met)

ALGORITHM 1: Basic DE algorithm

To begin with, a population of *NP* is randomly created. Each candidate in the population consists of *D* parameters and is represented as a *D*-dimensional vector. In our case, each candidate is a pair of *D*-dimensional vectors which include *b* coefficients and *a* coefficients. The magnitude response of the "Universal" FIR whitening filter is used to evaluate the candidates. During the iteration, each candidate in the population will go through mutation, crossover, evaluation and selection to approach the target.

- ***Mutation***

For parameter *j* of a candidate vector C_i , where *j* = 1, 2, …, *D*., a mutant parameter is produced by

$$P_{j,m,i} = P_{j,i} + K(P_{j,r,1} - P_{j,i}) + F(P_{j,r,2} - P_{j,r,3}), \qquad (1)$$

where $P_{j,r,1}$, $P_{j,r,2}$ and $P_{j,r,3}$ are parameters of candidates randomly selected from the population, such that all the candidates involved should not be identical to each other. *K* is the combination factor and *F* is the scaling factor which affects $(P_{j,r,2} - P_{j,r,3})$.

- ***Crossover***

The mutant candidate vector is mixed by the parent parameter and mutant parameter

$$P_{j,c,i} = \begin{cases} P_{j,m,i}, & if(rand_j \le CR) \; or \; j = cutpoint \\ P_{j,i}, & if(rand_j > CR) \; and \; j \ne cutpoint \end{cases}, \qquad (2)$$

where *CR* is the cross-rate which is less than 1 and greater than 0 and cut-point is a random number in the range of 1 to *D*, $rand_j \in [0,1]$. When the index *j* is equal to the cut-point or a crossover is triggered (a random number is less than or equal to cross-rate), mutant parameter is used, otherwise the parent parameter is used. *b* coefficients and *a* coefficients are going through this process separately. Hence, after this process a pair of mutant *b* and *a* coefficients is created.

- ***Evaluation***

To evaluate the performance of IIR filters designed, the magnitude response of the "Universal" FIR whitening filter, H_{FIR}, is compared to the magnitude response of IIR filters, $H_{IIR}(b,a)$, by computing the RMSE.

In our method, a lowpass filter with cutoff frequency *F* Hz is implemented to the whitening band limit filter. Compared with achieving a global minimum RMSE, achieving a RMSE at low level in the first *F* Hz while maintaining an overall RMSE that can be accepted is optimal in our case. Such being the case, the cost function is separated into two parts

$$E_i = w_1 \sqrt{\frac{1}{N_1} \sum_{k=1}^{N_1} (H_{FIR,k} - H_{IIR,k}(b,a))^2} +$$

$$w_2\sqrt{\frac{1}{N-N_1}\sum_{l=N_1+1}^{N}(H_{FIR,j}-H_{IIR,j}(b,a))^2}, \qquad (3)$$

where N is the number of samples of the magnitude response, w_1 is the weight of the first N_1 samples, w_2 is the weight of the remaining $N-N_1$ samples.

- ***Selection***

The cost of the original pair of b and a coefficients (before mutation), E_o, and the cost of mutant pair of b and a coefficients, E_m, are computed. If $E_o < E_m$, the original pair will be kept and the mutant pair will be discarded; if $E_o \geq E_m$, then the mutant pair will replace the original pair.

After certain number of iterations, the pair with minimum E will be selected as the final solution.

Performance Evaluation Method

To begin with, the selection of number of iterations is very important. Apparently, if the number of iterations is too small, the final solution can certainly be improved. If the number of iterations is too huge, running the whole process will be extremely time consuming, yet the performance of the optimal solution will only have tiny change after uncertain number of iterations depending on the random initialized population. So, it is necessary to determine an appropriate number of iterations. To solve this problem, several numbers of iterations were tested, and the results are shown in the following section.

To evaluate the performance of the desired "Universal" FIR whitening filter, the EMG-force method introduced in Chapter 2 was used, except that the original whitening filter or the "Universal" FIR whitening filter was replaced by the "Universal" IIR filter. The results are presented as mean ± std. dev of the RMSE between real torque and estimated torque.

III. IMPLEMENTATION AND RESULTS

DE Algorithm Implementation

A 2nd-order IIR highpass filter was designed, so each candidate (b and a coefficients)

has 3 parameters (although $a_0 = 1$), which is $D = 3$. To implement the DE algorithm, parameters were selected as following: the number of population is 100, $K = 0.8$, $F = 0.8$, cross-rate = 0.5, $F = 600$ Hz (the same as Chapter 2), $w_1 = 0.8$, $w_2 = 0.2$.

To determine the number of iterations, several numbers were selected. From 20 iterations to 300 iterations with an increment of 20 were tested. Each number of iterations was tested 10 times then computed the mean ± std. dev of the RMSE between the magnitude response of the achieved IIR filter and the "Universal" FIR whitening filter. The table below shows all the results.

TABLE I

THE PERFORMANCES OF 2ND-ORDER IIR FILTER DESIGNED BY DIFFERENT NUMBER OF ITERATIONS BY USING DE ALGORITHM.

Number of Iterations	RMSE (mean±std)
20	6.7781±1.8726
40	3.7391±0.6530
60	3.1199±0.3431
80	3.0033±0.5336
100	2.8448±0.3157
120	2.7722±0.0712
140	2.7700±0.1039
160	2.7387±0.0824
180	2.7176±0.0441
200	2.8943±0.3423
220	2.7585±0.0928
240	2.6960±0.0057
260	2.6971±0.0056
280	2.6955±0.0009
300	2.7043±0.0105

The table shows that the average RMSE decreases rapidly when the number of iterations is small (20 - 60), and doesn't change relativly when the number goes beyond 100. The figure below shows the results more graphically.

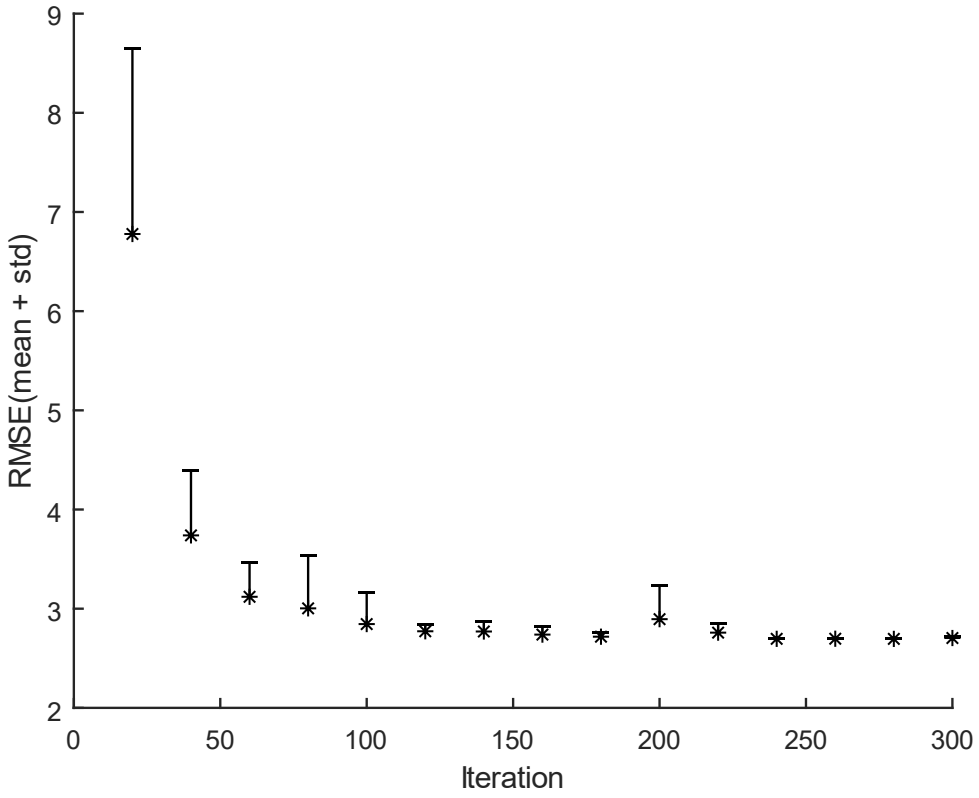

Fig. 1: The average RMSE + standard deviation between the magnitude response of optimal 2^{nd}-order IIR filter designed by different number of iterations and the magnitude response of "Universal" FIR whitening filter.

From the results, chosing 280 as the number of iterations is reasonable. The figure below shows the magnitude response of the designed IIR whitening filter (optimal after 280 iteraions) and the "Universal" FIR whitening filter.

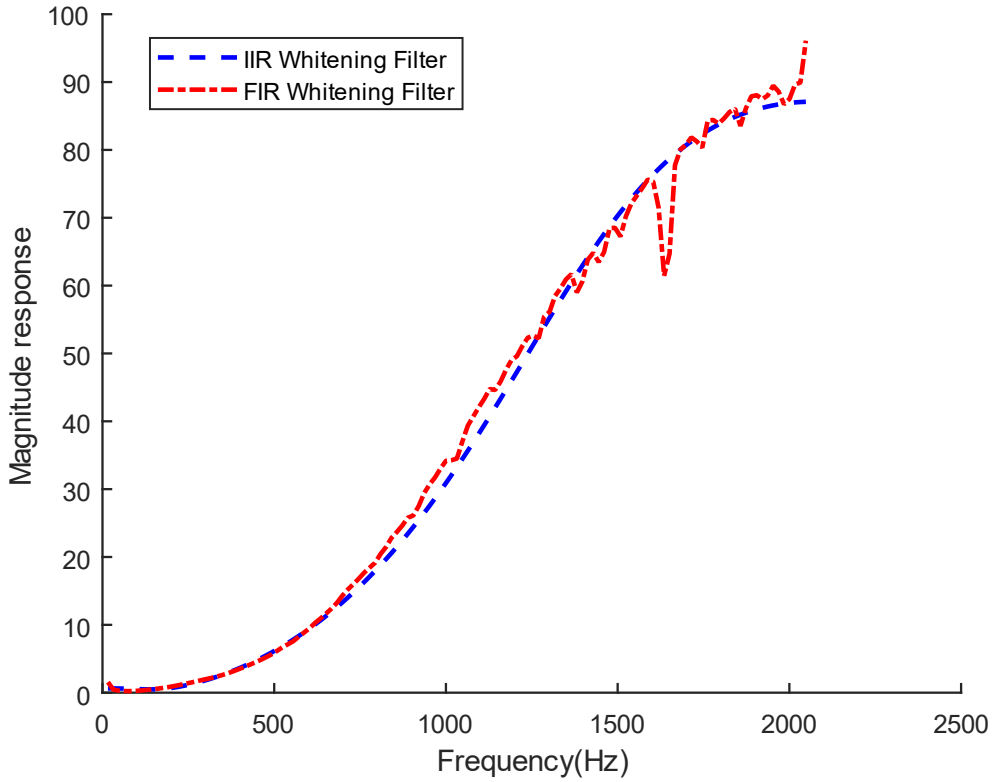

Fig.2: The magnitude response of "Universal" 2nd-order IIR and 60th-order FIR whitening filters.

IIR Filter Performances and results

To test the performance of the "Universal" IIR whitening filter, the whitening band limit frequency was varied from 200 Hz to 1400 Hz with an increment of 200 Hz; also 500 Hz and 700 Hz were tested because 600 Hz whitening band is the default value [17, 18] and performance around this value should be investigated.

The original adaptive whitening filter includes two major parts: stage 1, the fixed whitening shape; stage 2, adaptive noise canceler which is related to the noise [17]. So, the methods to test IIR whitening filter and compare it to the subject-specific whitening filter and FIR whitening filter are: replace the fixed whitening shape by using the magnitude response of IIR or FIR filter (replace stage 1) and replace stage 2 using average noise spectrum calibrated by using 64 subjects' 5 s noise data to replace the subject-specific noise.

Table below shows each method's EMG-force error (%MVC) results with different

whitening band limit frequencies.

TABLE II

THE PERFORMANCES OF DIFFERENT METHODS BY USING DIFFERENT WHITENING BAND LIMIT FREQUENCY.

Whitening band limit (Hz)	Method	RMSE (mean±std)
200	Original Whitened	5.48%±2.45%
	Unwhitened	5.5%±2.5%
	Universal FIR Whitened stage1 only	5.38%±2.38%
	Universal FIR whitened, stage1+average noise	5.37%±2.38%
	Universal IIR Whitened stage1 only	5.52%±2.41%
	Universal IIR whitened, stage1+average noise	5.48%±2.41%
400	Original Whitened	5.03%±2.11%
	Unwhitened	5.5%±2.5%
	Universal FIR Whitened stage1 only	4.90%±1.93%
	Universal FIR whitened, stage1+average noise	4.92%±2.05%
	Universal IIR Whitened stage1 only	5.02%±2.18%
	Universal IIR whitened, stage1+average noise	4.96%±2.17%
500	Original Whitened	4.92%±1.98%
	Unwhitened	5.5%±2.5%
	Universal FIR Whitened stage1 only	4.86%±1.96%
	Universal FIR whitened, stage1+average noise	4.86%±2.02%
	Universal IIR Whitened stage1 only	4.93%±2.07%
	Universal IIR whitened, stage1+average noise	4.88%±2.14%
600	Original Whitened	4.84%±1.98%
	Unwhitened	5.5%±2.5%
	Universal FIR Whitened stage1 only	4.81%±1.99%
	Universal FIR whitened, stage1+average noise	4.80%±2.03%
	Universal IIR Whitened stage1 only	4.84%±2.01%
	Universal IIR whitened,	4.81%±2.12%

	stage1+average noise	
700	Original Whitened	4.82%±2.02%
	Unwhitened	5.5%±2.5%
	Universal FIR Whitened stage1 only	4.81%±2.01%
	Universal FIR whitened, stage1+average noise	4.81%±2.07%
	Universal IIR Whitened stage1 only	4.83%±2.02%
	Universal IIR whitened, stage1+average noise	4.81%±2.14%
800	Original Whitened	4.82%±2.06%
	Unwhitened	5.5%±2.5%
	Universal FIR Whitened stage1 only	4.80%±2.04%
	Universal FIR whitened, stage1+average noise	4.80%±2.08%
	Universal IIR Whitened stage1 only	4.81%±2.04%
	Universal IIR whitened, stage1+average noise	4.80%±2.16%
1000	Original Whitened	4.77%±2.08%
	Unwhitened	5.5%±2.5%
	Universal FIR Whitened stage1 only	4.75%±2.04%
	Universal FIR whitened, stage1+average noise	4.77%±2.11%
	Universal IIR Whitened stage1 only	4.75%±2.02%
	Universal IIR whitened, stage1+average noise	4.78%±2.20%
1200	Original Whitened	4.75%±2.07%
	Unwhitened	5.5%±2.5%
	Universal FIR Whitened stage1 only	4.74%±2.06%
	Universal FIR whitened, stage1+average noise	4.74%±2.12%
	Universal IIR Whitened stage1 only	4.76%±2.05%
	Universal IIR whitened, stage1+average noise	4.79%±2.19%
	Original Whitened	4.75%±2.10%
	Unwhitened	5.5%±2.5%

1400	Universal FIR Whitened stage1 only	4.75%±2.05%
	Universal FIR whitened, stage1+average noise	4.74%±2.11%
	Universal IIR Whitened stage1 only	4.79%±2.08%
	Universal IIR whitened, stage1+average noise	4.80%±2.19%
1600	Original Whitened	4.76%±2.14%
	Unwhitened	5.5%±2.5%
	Universal FIR Whitened stage1 only	4.74%±2.06%
	Universal FIR whitened, stage1+average noise	4.73%±2.07%
	Universal IIR Whitened stage1 only	4.78%±2.10%
	Universal IIR whitened, stage1+average noise	4.79%±2.17%

To summarize all the results, several figures were made. Figures 3 and 4 are comparisons between subject-specific adaptive whitening filter (original whitening filter), FIR whitening filter and IIR whtiening filter. Figures 5, 6 and 7 are comparisons between whitening filters with different compositions: FIR whitening filter with universal shape only and universal shape plus average noise; IIR whitening filter with universal shape only and universal shape plus average noise.

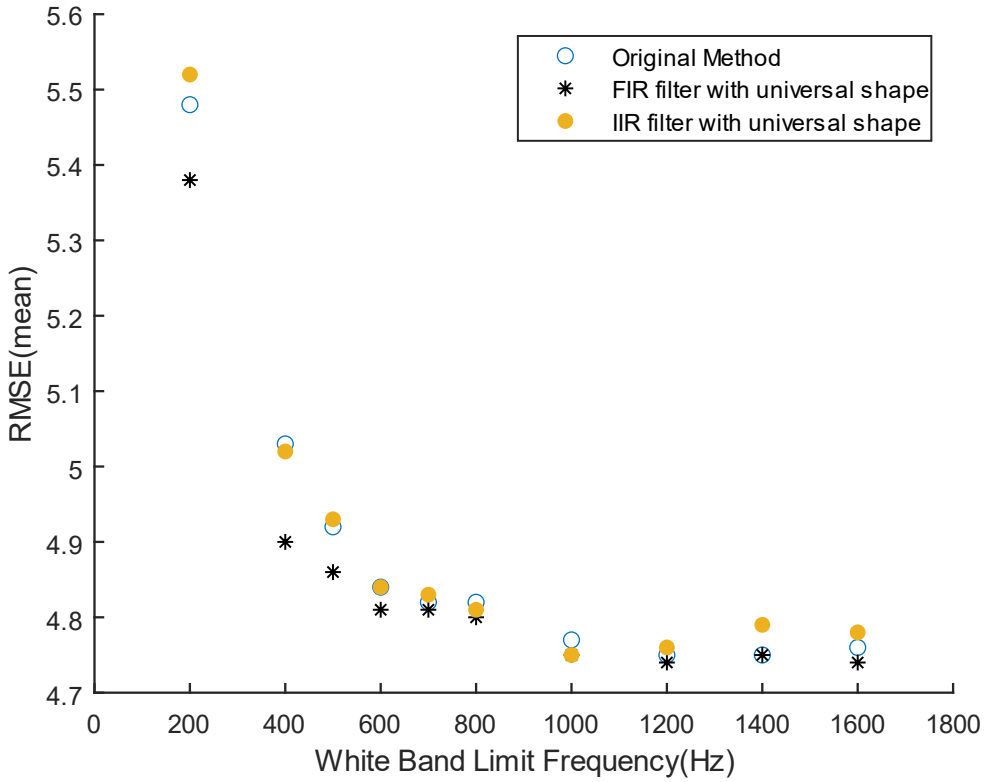

Fig. 3: Performances (mean RMSE of 64 subjects) comparison between subject-specific adaptive whitening filter and FIR filter only with universal shape and IIR filter only with universal shape.

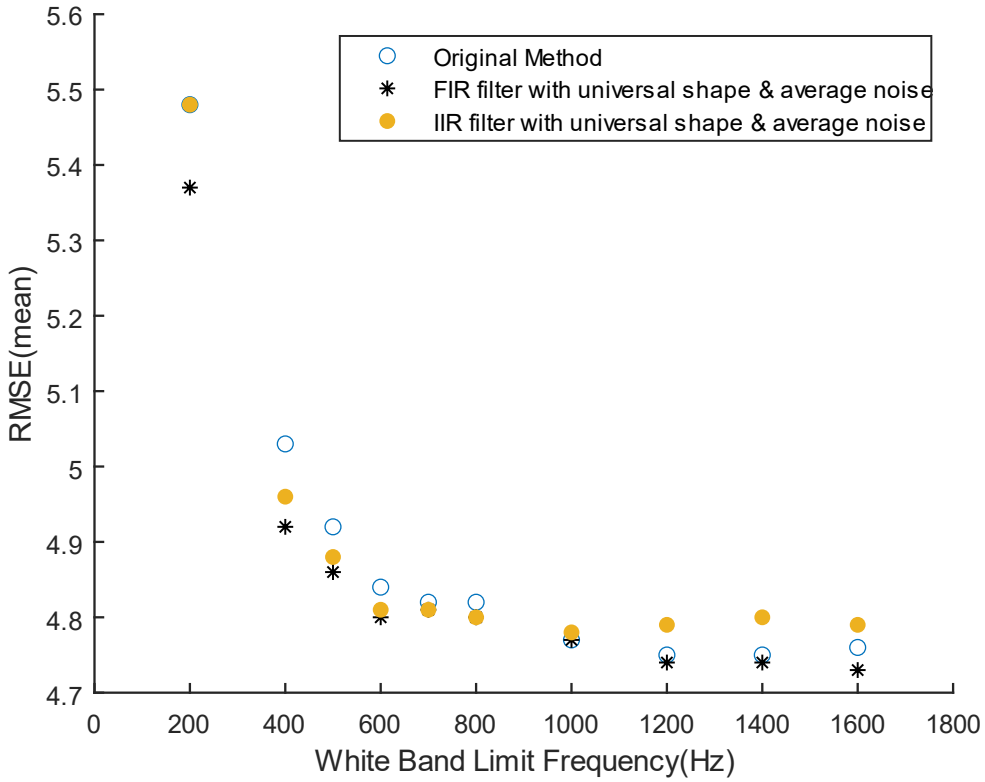

Fig. 4: Performances (mean RMSE of 64 subjects) comparison between subject-specific adaptive whitening filter and FIR filter with universal shape & average noise and IIR filter with universal shape & average noise.

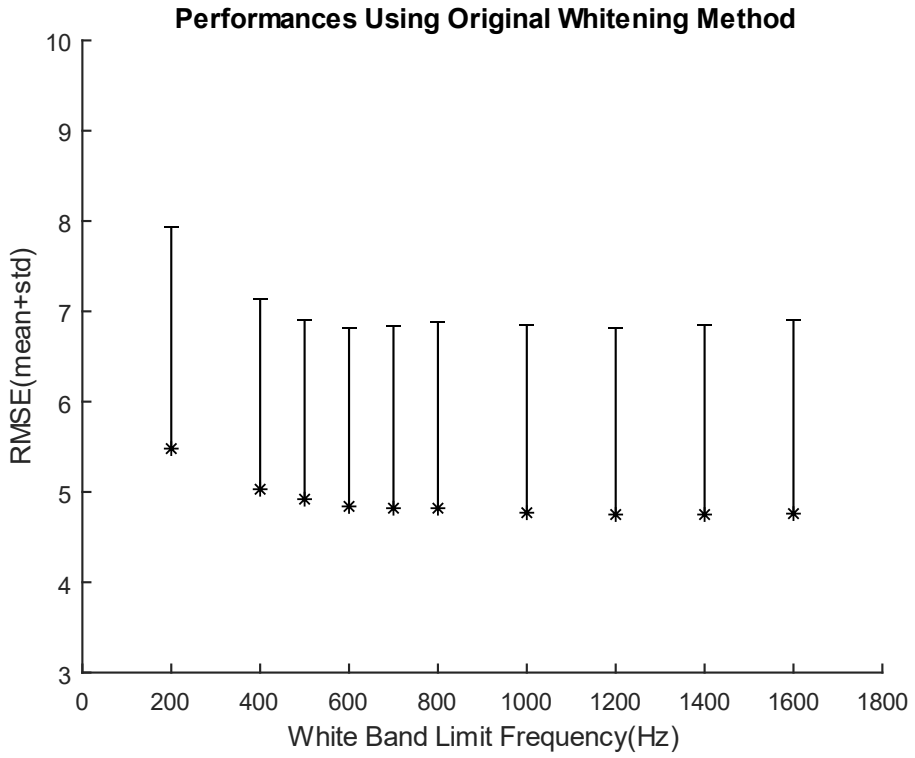

Fig. 5: Performances (mean + std. dev. RMSE of 64 subjects) of subject-specific adaptive whitening filter.

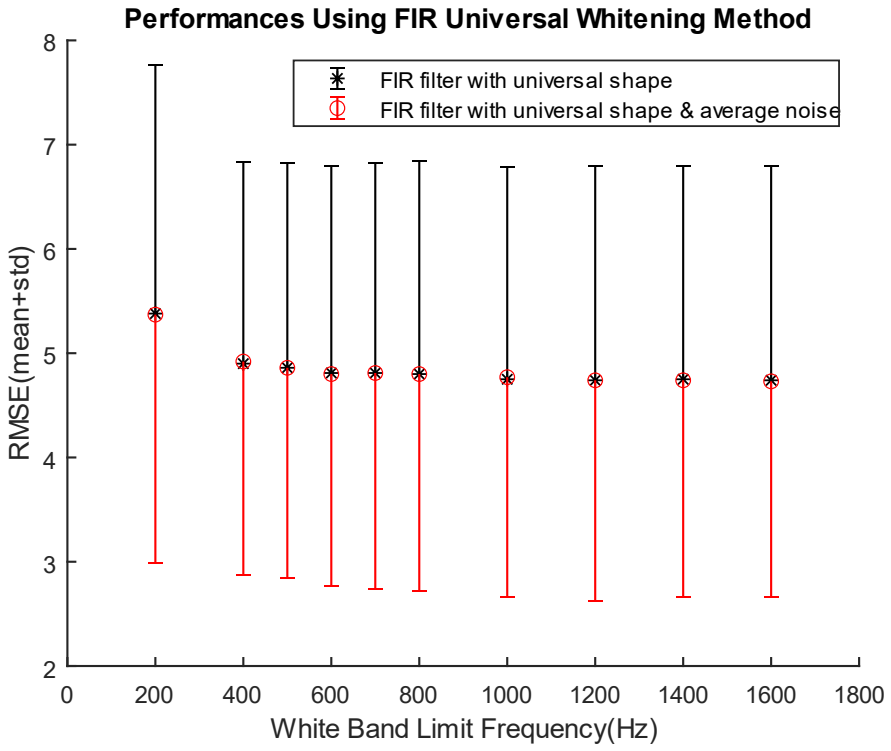

Fig. 6: Performances (mean + std. dev. RMSE of 64 subjects) between FIR filter with universal shape & average noise and FIR filter with universal shape only.

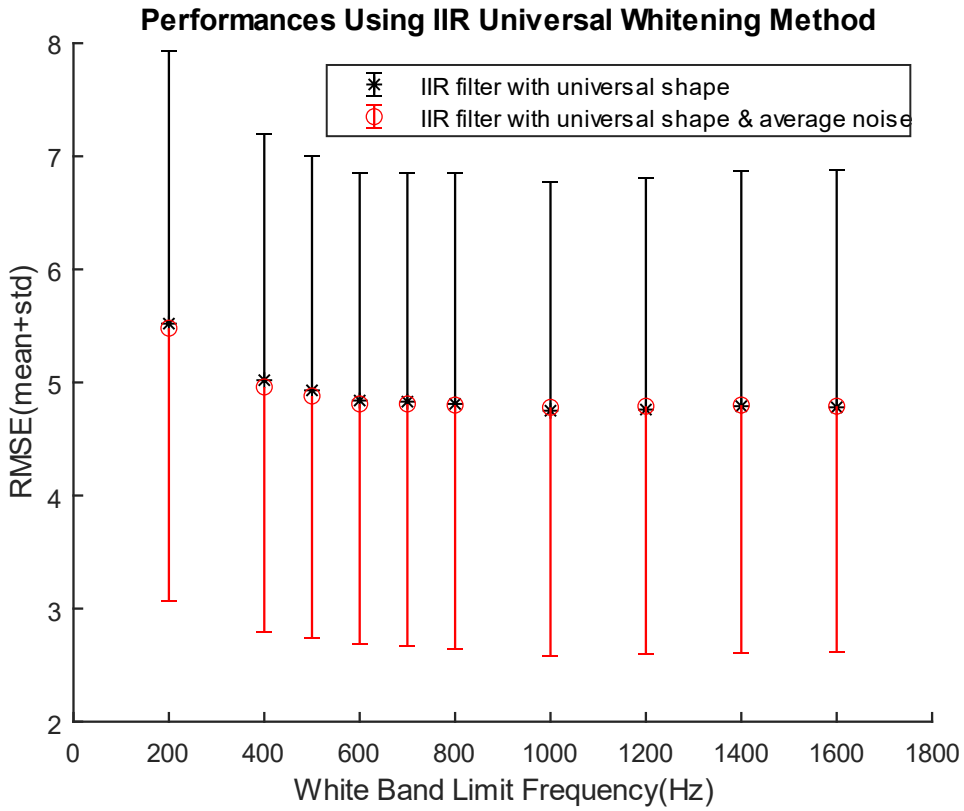

Fig. 7: Performances (mean + std. dev. RMSE of 64 subjects) between IIR filter with universal shape & average noise and IIR filter with universal shape only.

For statistical testing, the Shapiro-Wilk test was used to check whether the RMSEs formed a normal distribution. The results showed that all RMSEs from 5 different methods (original subject-specific whitening, "Universal" FIR whitening, universal shape with/without average noise spectrum, "Universal" IIR whitening, universal shape with/without average noise spectrum) are not parametric ($p < 0.05$). Such being the case, we chose Kruskal-Wallis H test (one-way ANOVA on ranks) which is commonly used when testing non-parametric data. The test results showed that there was no statistically significant difference in RMSE between the 5 methods used. We found $\chi^2(4) = 0.181$, $p = 0.996$, with a mean rank RMSE 160.69 for FIR whitening filter with stage 1 only, 158.89 for FIR whitening filter with both stage 1 and average noise spectrum, 162.16 for IIR whitening filter with stage 1 only, 157.31 for IIR whitening filter with both stage 1 and average noise spectrum and 163.45 for original subject-specific whitening filter.

IV. DISCUSSION

From results given above, the "Universal" IIR whitening filter designed by using DE algorithm has very similar performance compared with both subject-specific adaptive whitening filter and "Universal" FIR whitening filter.

For IIR filter with universal shape only, the overall performance becomes better as the whitening band limit frequency increases from 200 Hz to 1000 Hz, this trend is very similar to the performance of FIR filter with universal shape only and the subject-specific adaptive whitening filter [18]. However, when the whitening band limit is greater than 1000 Hz, the performance drops. Due to the weights selected in the cost function, the magnitude response beyond 600 Hz is given too much attention, so the drop of performance is expected. Hence, 600 Hz to 1000 Hz will be better choice for whitening band limit when implementing an IIR whitening filter.

IIR filter with universal shape and average noise has very similar performance compared to IIR filter with universal shape only. Using IIR filter with universal shape and average noise can simplify the traditional subject-specific adaptive whitening filter a lot with no loss in the performance. To be specific. A length of 60 order FIR filter requires 60 multiplies per sample, however, a second order IIR only requires 5 multiplies per sample.

REFERENCES FOR THIS CHAPTER

1. J.R.Potvin, "Less is more: high pass filtering, to remove up to 99% of the surface EMG signal power, improves EMG-based biceps brachii muscle force estimates," *Journal of Electromyography and Kinesiology*, vol 14, issue 3, pp 389-399, 2004.
2. J. J. Shynk, "Adaptive IIR filtering," *IEEE ASSP Magazine*, vol. 6, no. 2, pp. 4–21, 1989.
3. M. Radenkovic and T. Bose, "Adaptive IIR filtering of nonstationary signals," Si*gnal Processing*, vol. 81, no. 1, pp. 183–195, 2001.
4. S. D. Stearns, "Error surface of recursive adaptive filters," *IEEE Trans. Acoust., Speech, Signal Processing*, vol. 29, no. 3, pp. 763–766, 1981.
5. Nurhan Karaboga, "Digital IIR Filter Design Using Differential Evolution Algorithm," *EURASIP Journal on Advances in Signal Processing*, vol 2005, 1 January 2005, Pages 1269-1276.
6. N. Karaboga, A. Kalinli, and D. Karaboga, "Designing IIR filters using ant colony optimisation algorithm," *Journal of Engineering Applications of Artificial Intelligence*, vol. 17, no. 3, pp. 301–309, 2004.

7. R. Nambiar and P. Mars, “Genetic and annealing approaches to adaptive digital filtering,” *in IEEE 26th Asilomar Conference on Signals, Systems & Computers*, vol. 2, pp. 871–875, Pacific Grove, Calif, USA, October 1992.
8. S. Chen, R. H. Istepanian, and B. L. Luk, “Digital IIR filter design using adaptive simulated annealing,” *Digital Signal Processing*, vol. 11, no. 3, pp. 241–251, 2001.
9. J. Radecki, J. Konrad, and E. Dubois, “Design of multidimensional finite-wordlength FIR and IIR filters by simulated annealing,” *IEEE Trans. on Circuits and Systems II: Analog and Digital Signal Processing*, vol. 42, no. 6, pp. 424–431, 1995.
10. D. M. Etter, M. J. Hicks, and K. H. Cho, “Recursive adaptive filter design using an adaptive genetic algorithm,” *in IEEE International Conference Acoustics, Speech, Signal Processing (ICASSP ’82)*, vol. 7, pp. 635–638, Albuquerque, NM, USA, May 1982.
11. N. E. Mastorakis, I. F. Gonos, and M. N. S. Swamy, “Design of two-dimensional recursive filters using genetic algorithms,” *IEEE Trans. on Circuits and Systems I-Fundamental Theory and Applications*, vol. 50, no. 5, pp. 634–639, 2003.
12. K. S. Tang, K. F. Man, S. Kwong, and Q. He, “Genetic algorithms and their applications,” *IEEE Signal Processing Mag*., vol. 13, no. 6, pp. 22–37, 1996.
13. S. C. Ng, S. H. Leung, C. Y. Chung, A. Luk, and W. H. Lau, “The genetic search approach: a new learning algorithm for IIR filtering,” *IEEE Signal Processing Mag*., vol. 13, no. 6, pp. 38–46, 1996.
14. R. Thamvichai, T. Bose, and R. L. Haupt, “Design of 2-D multiplierless IIR filters using the genetic algorithm,” *IEEE Trans. on Circuits and Systems-I: Fundamental Theory and Applications*, vol. 49, no. 6, pp. 878–882, 2002.
15. A. Lee, M. Ahmadi, G. A. Jullien, R. S. Lashkari, and W. C. Miller, “Design of 1-D FIR filters with genetic algorithm,” *in Proc. IEEE International Symposium on Circuits and Systems*, vol. 3, pp. 295–298, Orlando, Fla, USA, May/June 1999.
16. R. Storn and K. Price, “Differential evolution—a simple and efficient adaptive scheme for global optimization over continuous spaces,” Tech. Rep. TR-95-012, International Computer Science Institute (ICSI), Berkeley, Calif, USA, March 1995.
17. Edward A. Clancy, “Adaptive Whitening of the Electromyogram to Improve Amplitude Estimation,” *IEEE Transactions on Biomedical Engineering*, Vol. 47, No. 6, pp. 709-719, 2000.
18. Meera Dasog, “Electromyogram Bandwidth Requirements When the Signal is Whitened, ” *IEEE Transactions on Neural Systems and Rehabilitation Engineering*, Vol. 22, No. 3, pp. 664–670, 2014.

CHAPTER 4 – OPTIMAL ESTIMATION OF EMG STANDARD DEVIATION (EMGσ) REQUIRES NOISE SUBTRACTION IN THE POWER DOMAIN: MODEL-BASED DERIVATIONS AND THEIR IMPLICATIONS

This chapter has been accepted as: Haopeng Wang, Kiriaki J. Rajotte, He Wang, Chenyun Dai, Ziling Zhu, Moinuddin Bhuiyan, Xinming Huang and Edward A. Clancy, "*Optimal Estimation of EMG Standard Deviation (EMGσ) in Additive Measurement Noise: Model-Based Derivations and their Implications*", *IEEE Transactions on Neural Systems and Rehabilitation Engineering*

***Abstract*—Typical electromyogram (EMG) processors estimate EMG signal standard deviation (EMGσ) via moving average root mean square (RMS) or mean absolute value (MAV) filters, whose outputs are used in force estimation, prosthesis/orthosis control, etc. In the inevitable presence of additive measurement noise, some processors subtract the noise standard deviation from EMG RMS (or MAV). Others compute a root difference of squares (RDS)—subtract the noise variance from the square of EMG RMS (or MAV), all followed by taking the square root. Herein, we model EMG as an amplitude-modulated random process in additive measurement noise. Assuming a Gaussian (or, separately, Laplacian) distribution, we derive analytically that the maximum likelihood estimate of EMGσ requires RDS processing. Whenever that subtraction would provide a negative-valued result, we show that EMGσ should be set to zero. Our theoretical models further show that during rest, approximately 50% of EMGσ estimates are non-zero. This result is problematic when EMGσ is used for real-time control, explaining the common use of additional thresholding. We tested our model results experimentally using biceps and triceps EMG from 64 subjects. Experimental results closely followed the Gaussian model. We conclude that EMG processors should use RDS processing and not noise standard deviation subtraction.**

***Index* Terms—Biological system modeling, biomedical signal processing, electromyogram, electromyogram (EMG) amplitude estimation, electromyography, myoelectric signal processing.**

I. INTRODUCTION

THE surface electromyogram (EMG) interference pattern has commonly been processed by the cascade operations of highpass filtering (to remove DC offsets and attenuate motion artifacts); optional pre-whitening [1-3]; and then taking its moving average root mean square (RMS), moving average mean absolute value (MAV), or by rectifying the signal followed by lowpass filtering. If EMG is modeled as an amplitude-modulated random process, then these schemes estimate its time-varying standard deviation (EMGσ). For constant-force, non-fatiguing contractions, it has been shown that RMS processing is the optimal estimate of EMGσ if the noise-free EMG signal is modeled as Gaussian distributed [2, 4-6], and that MAV processing is optimal if the noise-free EMG signal is modeled as Laplacian distributed [7]. EMGσ has been used to estimate torque [8-13] and mechanical impedance about a joint [14-19], in motor control research [20], and in applications including prosthesis control [21-23], ergonomics [24, 25] and biomechanics [26, 27].

However, EMG is always measured in the presence of additive measurement noise, i.e., noise that exists independent of the level of muscle effort. This noise arises from the measurement apparatus (thermal and active device noise), radiated electromagnetic interference, electrode-to-skin contact resistance [28], unrelated electrophysiological activity, etc. [29]. This noise has an average RMS intensity that is 1.1–4.5% of the RMS EMG at maximum voluntary contraction (MVC) [3, 8, 9, 30-34]. Consequently, the signal to noise ratio (SNR) is low at low contraction levels.

Thus, researchers have proposed alterations to their EMG processors and/or models to include noise. Kaiser and Peterson [1] found that the shape of their whitening filter should be a function of the contraction level, with lower high-frequency gain during

low contraction levels. Parker et al. [35-37] modeled noise as an additive (white Gaussian) process when solving for an optimal multistate EMG classifier, and when analyzing (but not solving) EMGσ estimators. This additive noise model is now common (e.g., [3, 38-40]). Clancy and Farry [3] whitened the raw EMG, then attenuated additive noise using an adaptive Wiener filter. A Weiner filter is the optimal linear filter for attenuating additive noise, but is not necessarily the optimal filter overall. Many papers within the ergonomics literature routinely subtract the standard deviation of the background noise from RMS (or MAV) estimates [41]. However, it has been theoretically argued [42, 43] that the root difference of squares (RDS) [i.e., subtracting the noise variance from the square of EMG RMS (or MAV), all followed by taking the square root] is the correct approach. An experimental comparison found that RDS processing performs better than standard deviation subtraction [44].

The argument for RDS processing is based on the fact that if the signal and noise are independent, then their variances add—in theory. However, to our knowledge, this proposed processor has not been derived (i.e., solved for, based on a model) as a statistical estimator in the published literature (although one unpublished preliminary result appears in [45]). Solution via an estimator can demonstrate the optimality (or lack thereof) of a processor and expose its statistical properties. Herein, we provide this derivation, some of its properties and experimental evaluation of the derived optimal results, all for the case of constant-effort contraction.

II. Mathematical Models of EMG in Additive Noise

Consider an amplitude modulated model of the measured EMG signal, *m[n]*, during constant-effort contraction as [2, 5, 35-37]:

$$m[n] = s \cdot x[n] + v[n], \quad 0 \le n < N \qquad (1)$$

where n is the discrete-time sample index, $s \equiv EMG\sigma$ is the standard deviation (i.e., modulation) of the noise-free EMG, $(s \cdot x[n])$ is the noise-free EMG signal and $v[n]$ is additive noise. Let $x[n]$ be zero mean, unit-variance, wide-sense stationary,

correlation-ergodic and have independent samples (i.e., via pre-whitening). Let $v[n]$ be similarly specified, but of variance equal to q^2 and independent of $x[n]$. Let $\underline{m}$, $\underline{x}$ and $\underline{v}$ be vectors comprised of *N* samples of each respective random variable.

Gaussian Model—EMGσ Estimate [45, 46]

Let both $\underline{x}$ and $\underline{v}$ be jointly Gaussian. Then, $\underline{m}$ is jointly Gaussian with zero mean and covariance matrix: $K_{\underline{mm}} = \sigma_m^2 \, I$, where $\sigma_m^2 = s^2 + q^2$ and I is the identity matrix. Thus, the probability density function (PDF) for $\underline{m}$, given that the standard deviation of the noise-free EMG is $s \equiv EMG\sigma$, is:

$$p_{\underline{m}|s}\left(\underline{M}|s\right) = \frac{e^{\frac{-\underline{M}^T K_{\underline{mm}}^{-1} \underline{M}}{2}}}{(2\pi)^{N/2}\left|K_{\underline{mm}}\right|^{1/2}} = \frac{e^{\frac{-\sum_{n=0}^{N-1} M^2[n]}{2(s^2+q^2)}}}{[2\pi(s^2+q^2)]^{N/2}}, \qquad (2)$$

where $\underline{M}$ denotes an instance of the random vector $\underline{m}$.

The maximum likelihood (ML) estimate of s is the value $\hat{s}$ which maximizes the above PDF. A monotonic transformation of the PDF does not alter the location of the maximum. Thus, taking the natural logarithm yields:

$$\ln\left[p_{\underline{m}|s}\left(\underline{M}|\hat{s}\right)\right] = -\frac{N}{2}\ln(2\pi) - \frac{N}{2}\ln(\hat{s}^2 + q^2) - \frac{\sum_{n=0}^{N-1} M^2[n]}{2(\hat{s}^2+q^2)}. \quad (3)$$

Differentiating the above with respect to $\hat{s}$ gives:

$$\frac{\partial \ln\left[p_{\underline{m}|s}\left(\underline{M}|\hat{s}\right)\right]}{\partial \hat{s}} = -\frac{N}{2}\frac{2\hat{s}}{\hat{s}^2+q^2} + \frac{\hat{s}\sum_{n=0}^{N-1} M^2[n]}{(\hat{s}^2+q^2)^2}. \qquad (4)$$

Setting this derivative to zero and manipulating leads to a quadratic equation for $\hat{s}^2$, the square root of which provides our intermediate result. The quadratic equation has two solutions. But, one of these solutions is not real-valued, so can be eliminated. The retained intermediate result, written as a discrete-time filter, is:

$$\hat{s}[n] = \sqrt{\left(\frac{\sum_{i=0}^{N-1} M^2[n-i]}{N}\right) - q^2}. \qquad (5)$$

The parenthesized term within the square root is the mean square value. Hence, the noise correction is made via RDS processing.

The second derivative of (3) with respect to $\hat{s}$, evaluated at the location of the intermediate result specified by (5) is:

$$\frac{\partial^2 \ln\left[p_{\underline{m}|s}\left(\underline{M}|\hat{s}\right)\right]}{\partial\, \hat{s}^2} = \left[\frac{2\,N^3}{\left(\sum_{i=0}^{N-1} M^2[n-i]\right)^2}\right]\left[q^2 - \frac{\sum_{i=0}^{N-1} M^2[n-i]}{N}\right]. \quad (6)$$

This second derivative is less than or equal to zero, indicating a local maximum (and not a minimum), when $\frac{1}{N}\sum_{n=0}^{N-1} M^2[n-i]$ exceeds the noise variance q^2. This condition is almost always satisfied during active muscle contraction, but not during low-level contractions or rest. When the condition is not satisfied, maximization with respect to $\hat{s}$ of the PDF occurs at the boundary constraint where $\hat{s} = 0$ [47]. Hence, the complete solution for this ML estimate is:

$$\hat{s}_{\mathrm{RMS}}[n] = \sqrt{\max\left[0,\ \left(\frac{\sum_{i=0}^{N-1} M^2[n-i]}{N}\right) - g^2 q^2\right]}, \quad (7)$$

where "max" denotes the maximum value operator and the "RMS" subscript emphasizes the use of an RMS processor. Constant scaling factor g has been inserted into this solution, since some applications prefer to artificially inflate the noise threshold. For example, in myoelectric prosthesis control, g > 1 helps to insure that the prosthesis is not actuated during rest. For the optimum ML estimate, g = 1.

Denote the term in the rounded parenthesis of (7) (i.e., the mean square value of the measured EMG signal) as y. This random variable is Gamma distributed as:

$$p_y(Y) = \frac{Y^{\frac{N}{2}-1}\, e^{\frac{-Y\cdot N}{2\sigma_m^2}}}{\left(\sigma_m\sqrt{\frac{2}{N}}\right)^N \Gamma\left(\frac{N}{2}\right)}\, \mu(Y), \quad (8)$$

where $\Gamma(\cdot)$ is the Gamma function and $\mu(\cdot)$ is the step function. Its cumulative density function (CDF) is:

$$P_{y\leq}(Y) = 1 - \sum_{k=0}^{\frac{N}{2}-1} \frac{\left(\frac{N}{2\,\sigma_m^2}\right)^k Y^k\, e^{\frac{-Y\cdot N}{2\sigma_m^2}}}{k!}\, \mu(Y)\,, N \text{ even}. \quad (9)$$

When the muscle is at rest, the true EMGσ is zero $(s = 0)$ and the variance of the measured EMG signal is $\sigma_m^2 = q^2$. A fraction of the EMGσ estimates—but not all—will be zero (due to the noise variance subtraction). This probability of estimating a zero value during rest is the CDF of y, evaluated at $Y = g^2 q^2$ (with $s = 0$). This probability, for N even, is:

$$P_{y\leq g^2q^2,Rest}(Y) = \left[1 - \sum_{k=0}^{\frac{N}{2}-1} \frac{\left(\frac{N}{2}\right)^k \; g^{2k} \; e^{\frac{-g^2N}{2}}}{k!}\right] \mu(Y). \quad (10)$$

Note that this probability is not a function of the noise variance and is only a function of N and g. Fig. 1 shows this probability as a function of N for four possible values of g. Equation 10 and Fig. 1 show that for $g > 1$, a negative-valued subtraction result within (7) is more likely, producing a higher probability of estimating $\hat{s} = 0$. Conversely, for $g < 1$, a negative-valued subtraction result is less likely, producing a lower probability of estimating $\hat{s} = 0$.

Laplacian Model—EMGσ Estimate [7, 45, 46]

MAV processing has been shown to be the ML estimate of EMGσ if the PDF is Laplacian [7]. So that the additive noise model has a Laplacian PDF, we directly model the measured EMG samples *m[n]* as being independent and of a Laplacian PDF—without explicit specification of the PDFs of *x[n]* and *v[n]*. (Note that if *x[n]* and *v[n]* are each modeled as Laplacian, then their sum is *not* Laplacian.) Nonetheless, if *x[n]* and *v[n]* are assumed independent, then their variances again add. Thus, the measured EMG again has variance: $s^2 + q^2$, and the PDF for sample *m[n]* is [48]:

$$p_{m[n]|s}(M[n]|s) = \frac{\sqrt{2}}{2} \cdot \frac{e^{\frac{-\sqrt{2}}{(s^2+q^2)^{1/2}}|M[n]|}}{(s^2+q^2)^{1/2}}. \quad (11)$$

Since the samples of the EMG vector $\underline{m}$ are independent, its joint PDF is the product of the *N* individual PDFs, which simplifies to:

$$p_{\underline{m}|s}(\underline{M}|s) = \left[\frac{\sqrt{2}}{2\,(s^2+q^2)^{1/2}}\right]^N e^{\frac{-\sqrt{2}}{(s^2+q^2)^{1/2}} \sum_{n=0}^{N-1}|M[n]|}. \quad (12)$$

Similar to the Gaussian case above, maximum likelihood estimation of s is found by taking the natural logarithm of the PDF, differentiating with respect to $\hat{s}$, setting this derivative to zero and solving for $\hat{s}$. Again, the second derivative proves this result to, in fact, be a minimum, subject to the same boundary constraint where $\hat{s} = 0$. The complete filter for this estimator, again inserting a scaling factor g for the noise, is:

$$\hat{s}_{MAV}[n] = \sqrt{\max\left[0, \left\{\left(\frac{\sqrt{2}}{N}\sum_{i=0}^{N-1}|M[n-i]|\right)^2\right\} - g^2q^2\right]}. \quad (13)$$

Denote the term in the curly brackets of (12) as *w*. The PDF for this random variable is:

$$p_w(W) = \frac{e^{-\frac{N\sqrt{W}}{\sigma_m}}}{2} \cdot \left[\sum_{k=0}^{N-1}\left(\left\{\frac{N}{\sigma_m\sqrt{W}} - \frac{(N-1-k)}{W}\right\} \cdot \prod_{p=1}^{N-1-k}\left\{\frac{N\sqrt{W}}{\sigma_m p}\right\}\right)\right] \mu(W).$$

(14)

Its CDF is:

$$P_{w\leq}(W) = \left\{1 - e^{-\frac{N\sqrt{w}}{\sigma_m}}\left[\sum_{k=0}^{N-1}\left(\prod_{p=1}^{N-1-k}\frac{N\sqrt{W}}{\sigma_m p}\right)\right]\right\}\mu(W). \quad (15)$$

The probability of estimating a zero value during rest is the CDF evaluated at $W = g^2q^2$ (with $s = 0$):

$$P_{w\leq g^2q^2,Rest}(W) = \left\{1 - e^{-Ng}\left[\sum_{k=0}^{N-1}\left(\prod_{p=1}^{N-1-k}\frac{Ng}{p}\right)\right]\right\}\mu(W). \quad (16)$$

Again, the probability of a zero value is only related to *N* and *g*. Fig. 1 shows this probability as a function of *N* for four possible values of *g*.

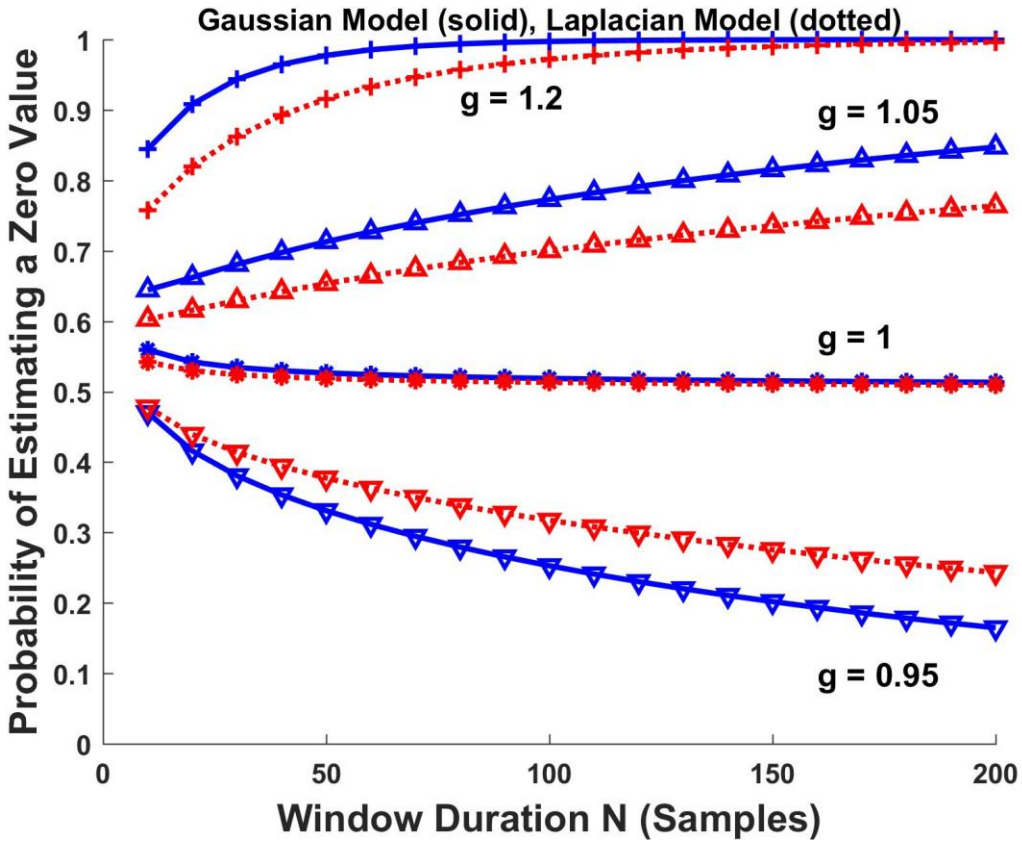

Fig. 1. Probability of estimating a zero EMGσ value during rest for theoretical Gaussian model (moving average RMS processing; solid blue) and Laplacian model (moving average MAV processing; dashed red) as a function of number of independent samples N, for four different noise gain values "g".

III. Experimental Evaluation of the Models

Experimental Data Set

Data from 64 subjects acquired during four prior experiments with overlapping protocols were used for this study [3, 8, 30, 33]. Re-analysis of these data was exempted from human studies supervision by the WPI Institutional Review Board. Subjects had no known neuromuscular deficits of the right shoulder, arm or hand. In each experiment (see Fig. 1 in [8] for a photograph of the most recently used experimental apparatus), a subject was seated and secured with seat belts. Their right shoulder was abducted 90o, elbow flexed 90o, and hand supinated perpendicular to the floor. Their wrist was cuffed to a load cell to measure constant-posture elbow torque.

The skin above the triceps and biceps muscles was scrubbed with an alcohol wipe. Gel was applied in the latter two studies. Four bipolar EMG electrode-amplifiers were secured over each of the triceps and biceps muscles, in a tightly-spaced transverse row centered on the muscle mid-line, midway between the elbow and the midpoint of the upper arm. Each electrode-amplifier had stainless steel, hemispherical contacts of diameter 4 or 8 mm, separated 10 mm edge-to-edge, oriented along the long axis of the muscle. A reference electrode was secured alongside the active electrodes. Each EMG channel had selectable gain, a CMRR $\geq$ 90 dB at 60 Hz, a 10 or 15 Hz highpass filter (second or fourth order), and a 1800 or 2000 Hz lowpass filter (fourth order). EMG and load cell data were sampled at 4096 Hz at 16-bit resolution. Achieved force was fed back in a real-time display, along with a force target.

After a brief warm-up, separate elbow flexion and extension maximum voluntary contraction (MVC) forces were measured, without the use of force feedback. At least

20–30 minutes had elapsed between the time at which the electrodes were mounted and the completion of these MVC measurements. Then, constant-force 50% MVC extension trials, 50% MVC flexion trials and 0% MVC trials (arm at rest, removed from the wrist cuff) were acquired for 5 s each, using force feedback. (Only one of each type of trial was used in our analysis.) Two or three minutes of rest was provided between trials to avoid cumulative fatigue. Each of the eight, 5-s duration EMG signals from a trial was defined as an "epoch." Before any further use off-line, each epoch was highpass filtered (15 Hz cut-off, fourth-order Butterworth); IIR notch filtered at 60 Hz and its harmonics (second-order); when selected, adaptively pre-whitened [3, 49]; and bandlimited to 600 Hz [50] (fourth-order Butterworth lowpass). Then the first 500 ms of each epoch was omitted to account for filter start-up transients.

Evaluating Model Assumptions—EMG PDF

We evaluated the model assumptions related to the first-order PDF of EMG, both at rest and during 50% MVC trials, with and without whitening. During 50% extension trials, only the four epochs from triceps electrodes were examined; during 50% flexion trials, only the four epochs from biceps electrodes were examined. A total of 512 epochs (64 subjects x 8 electrodes/subject) were available at 0% (rest) and at 50% MVC (combining extension and flexion). Each EMG epoch was normalized to a sample variance of one and a histogram PDF estimate formed (500 bins, equally spaced over the range from –5 to +5). The ensemble histogram sample means and standard deviations are shown in Fig. 2.

Best matching between the ensemble vs. theoretic Gaussian/Laplacian PDFs did not occur when using theoretic PDFs of unit variances. Thus, the absolute error difference between each ensemble and theoretic PDF was computed for theoretic PDF standard deviations between 0.5 and 2 (increment of 0.01). The minimum area and its corresponding theoretic PDF standard deviation are shown in Table I (see also Fig. 2). In all cases, the data more closely followed the Gaussian model. Kolmogorov-Smirnoff tests between the experimental ensemble PDFs and each of the Gaussian and Laplacian PDFs were not sensitive, finding no statistically significant differences using either the

Gaussian model (p > 0.99) or the Laplacian model (p > 0.31), for the four combinations of effort level (0% MVC, 50% MVC) and whitening. Thus, we computed the absolute area difference between each of the 512 histogram PDF estimates vs. the Gaussian/Laplacian PDFs, finding the best fit standard deviation for each. Paired sign tests (Bonferroni corrected) found the Gaussian PDF to be a better fit $(p < 10^{-6})$ for each of the four combinations.

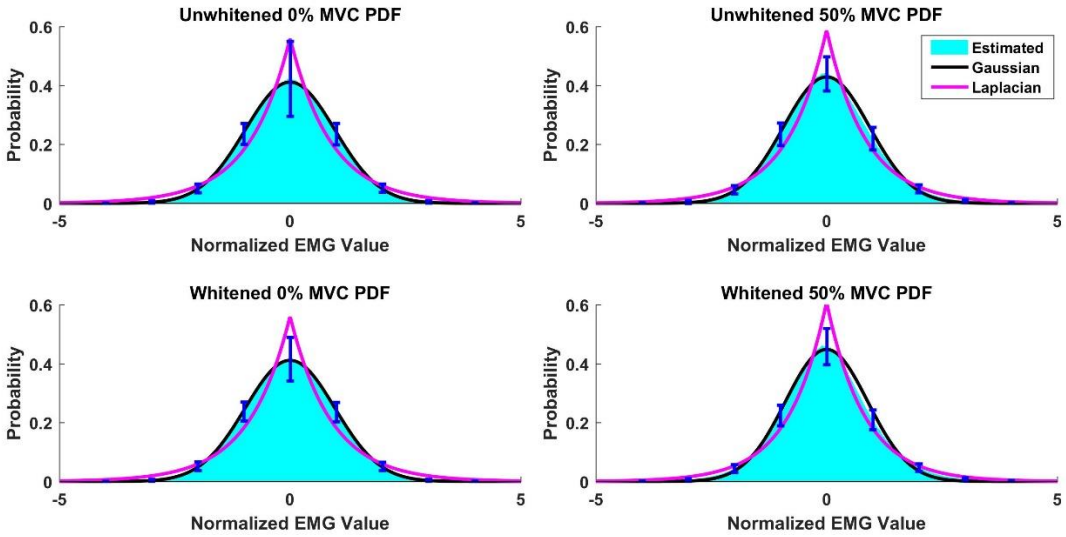

Fig. 2. Top shows ensemble-average (±1 std. dev.) PDF estimates of unwhitened EMG during 0% MVC (left) and 50% MVC (right), as well as best-fit theoretic Gaussian and Laplacian PDFs. Bottom shows corresponding PDF estimates from whitened EMG. N = 512 recordings from 64 subjects.

TABLE I
ABSOLUTE AREA DIFFERENCES BETWEEN EXPERIMENTAL ENSEMBLE PDFS AND GAUSSIAN/LAPLACIAN PDFS. PARENTHESES LIST STANDARD DEVIATION AT WHICH AREA DIFFERENCE WAS ASSESSED.

EMG	Gaussian Model		Laplacian Model	
Processing	0% MVC	50% MVC	0% MVC	50% MVC
Unwhite	0.0241 (0.97)	0.0530 (0.93)	0.1981 (1.26)	0.1730 (1.20)
White	0.0188 (0.97)	0.0749 (0.89)	0.2035 (1.26)	0.1532 (1.16)

Evaluating Estimates of EMGσ

Historically, quantitative evaluation of constant-effort EMGσ has used the ratio of the estimate mean to its standard deviation (the inverse of the coefficient of variation), denoted the SNR. With this definition, variations about the mean of EMGσ are

considered as “noise.” This definition was convenient, as knowledge of neither the “true” EMGσ value nor the EMGσ-force relationship was necessary, and the measure is invariant to signal gain. However, that definition is not as indicative of EMGσ estimate performance once additive noise is modeled. In particular, the noise can cause the EMGσ estimate to incorrectly coalesce about the wrong mean value. In this case, SNR would measure the variation of the processed signal plus noise; and not the desired error with respect to the true (noise-free) EMGσ—which is more appropriate for this study.

Thus, root mean square error between the true and estimated EMGσ value was used as the error measure. However, the true value is not known when assessing with real EMG data. Thus, we pursued an approach similar to [41]. Our available 50% MVC trials assume that muscle effort—and therefore EMGσ—is not changing during the contraction. So, we optionally whitened each EMG epoch, then normalized each 0% and, separately, each 50% MVC epoch to have a standard deviation of one. We treated each 50% MVC epoch as the “true” EMG signal and its 0% MVC epoch from the corresponding electrode as noise. We then multiplied each normalized 50% MVC EMG epoch point-by-point by a ramp (1 s zero, 3 s ramping from 0 to 0.1, 1 s at 0.1). To this signal, we added 0.02 times the respective, normalized 0% MVC epoch. This addition gave a SNR of 5, which is representative of measured EMG [3, 8, 9, 30-34]. We then computed the EMGσ estimate using a 200 ms duration centered (non-causal) window, only using RMS processing (since the Gaussian model was a much better fit to our data), with and without RDS processing. The root mean square error between the EMGσ estimate and the “true” EMGσ (i.e., the ramp pattern) was computed at times 1.0, 1.5, … 4.0 s across the 512 epochs (64 subjects x 8 electrodes per subject). Fig. 3 shows summary results. Due to non-normality of the data, we computed paired sign tests (separately for each time) between the root mean square error of all six unique paired combinations of the four factors: unwhitened data, whitened data, without RDS processing, and with RDS processing (Bonferroni corrected). Comparing each method with RDS processing to each method without RDS processing (four comparisons) always resulted in significantly lower errors with RDS processing for times $\leq$ 2.5 s

($p < 10^{-5}$), and no differences for times ≥ 3 s ($p > 0.1$). When unwhitened vs. whitened processors were compared without RDS processing (one combination), there were no statistical differences ($p > 0.1$), except at 1.5 s ($p = 10^{-4}$)—likely an anomoly. When unwhitened vs. whitened processors were compared with RDS processing (one combination), whitening had lower error for times ≤ 1.5 s ($p < 10^{-5}$), and was not significantly different for times ≥ 3.0 s ($p > 0.1$).

Evaluating Probability of a Zero Value at Rest

The theoretical results predict that the probability of estimating a zero value for EMGσ during rest is a function of the window length and the noise gain factor "g". We experimentally evaluated this result using the 512 0% MVC epochs. We again limited analysis to RMS processing. We computed the fraction of zero-valued estimates when using RDS processing for all combinations of: unwhitened vs. whitened processing, window length values ranging from N=2–400 ms, and g values of 0.95, 1, 1.05 and 1.2. The sample variance of each rest epoch was computed (after removing a 400 ms startup transient) and used as the noise variance q^2 to compute its respective RMS estimate of EMGσ.

With this method, the selected window length is misleading for comparison to the theoretical results shown in Fig. 1, because the experimental EMG signal is correlated (i.e., has finite bandwidth). To resolve this conflict, Bendat and Piersol [4, 51] list the number of effective independent samples for a correlated Gaussian process as: $N_{Eff} = 2B_S T$, where B_S is statistical bandwidth (Hz) and T is the window duration (s). Thus, we used the method of [52] to estimate statistical bandwidth from the PSD estimate of each 0% MVC epoch, separately with and without whitening (Welch method, Hamming window, 50% overlap, 614-length DFT). Without whitening we found the 0% MVC bandwidth to be $B_{S,Unwhite} = 118 \pm 72\ Hz$, and with whitening we found the 0% MVC bandwidth to be $B_{S,White} = 329 \pm 157\ Hz$. Fig. 4 plots the fraction of zero values during rest as a function of N_{Eff} and "g".

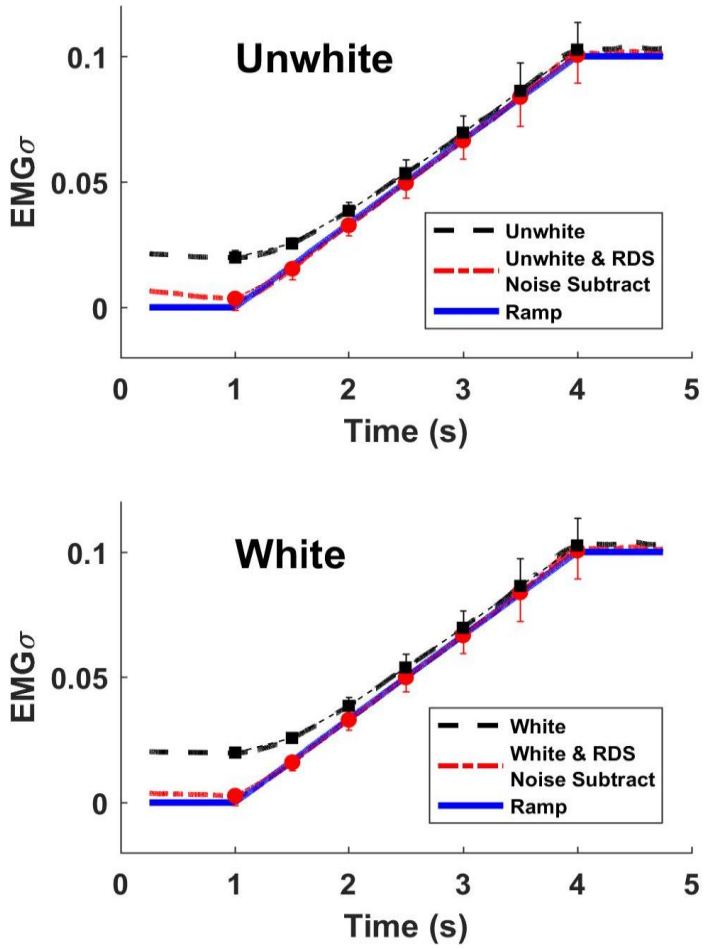

Fig. 3. Top shows ensemble averaged unwhitened EMGσ estimates along the ramp contraction, with and without noise subtraction. Symbols and one-sided error bars show mean and one standard deviation at times 1.0, 1.5, 2.0, …, 4.0. Bottom shows corresponding results for whitened EMGσ estimates.

IV. Discussion

Maximum Likelihood Estimates of EMGσ

There has been debate in the literature as to the best way in which to suppress the influence of additive noise when estimating EMGσ. While RDS processing has been suggested (as well as other approaches), no model-derived optimal solution has been peer-review published. Herein, we analytically derived, using maximum likelihood estimation, that constant-effort EMG, modeled as either a Gaussian or Laplacian

random process, requires RDS processing when additive noise is modeled [equations (7) and (13), respectively, with $g = 1$]. Further, our work shows that when the particular instance of the EMG signal is such that RDS processing would result in a negative value within the square root, then EMGσ should be estimated as EMGσ = 0. While these formulae are derived with constant-effort assumptions, existing EMG processors assume a quasi-stationary EMG signal, even during highly dynamic contractions [30, 53-56]. Thus, a moving average window assumes a constant EMGσ within that window, but an EMGσ that slowly varies between adjacent windows. Hence, these RDS processing results remain valid.

EMG Probability Density Function

It does not appear that the PDF of rest EMG has previously been reported. We found this PDF to closely match the Gaussian PDF.

But, the literature has variously reported the PDF of active EMG as Gaussian or as more peaked near zero than Gaussian (e.g., Laplacian), mostly in small sample size studies. Roesler [57] (sample size not listed, perhaps one subject; biceps, triceps and forearm muscles) found the EMG PDF to be precisely Gaussian across a range of isometric contraction levels. Parker et al. [35] (sample size not listed, likely one trial reported; intramuscular fine wires within the long head of the biceps brachii) found the EMG PDF to be Gaussian during an ~25% MVC and a just perceptible contraction. Hunter et al. [58] (one subject; biceps brachii muscle) found 30% MVC to have a PDF that is more peaked than Gaussian, as did Bilodeau et al. [59] for 20% MVCs (16 subjects; biceps brachii and brachioradialis muscles). Nazarpour et al. [60] (four subjects; abductor pollicis brevis and flexor carpi radialis muscles) found evidence that the PDF was more peaked (i.e., closer to Laplacian) at low level contractions, but more bell-shaped/Gaussian at higher contraction levels. They postulated that, since more motor unit firings contribute to the EMG during higher contraction levels, the interference signal more closely obeys the central limit theorem—resulting in a more Gaussian shape.

Our own prior work [7] (24 subjects; all distinct from the subjects in the present study)

found the PDF from biceps and triceps muscle EMG to be closer to Gaussian than Laplacian, for 10, 25, 50 and 75% constant-force MVCs, using apparatus and methods quite similar to that of the present study. However, this work found that MAV processing produced a higher SNR than RMS processing. A simulation study of constant-effort EMG confirmed that as the EMG PDF is progressively varied from Laplacian to Gaussian, there exists a region wherein the data are more Gaussian in distribution, but MAV processing performs better than RMS.

The present study likely reports the largest sample size to-date. Our EMG exhibited a distribution that closely matched the Gaussian PDF, with a poorer fit to the Laplacian PDF. Since our data were from 50% MVCs (a high contraction level), this result is consistent with the findings of Nazapour et al. [60]. Future comparison to data at lower contraction levels (in which [60] found a more peaked PDF) may be appropriate. The similarity in PDF shapes to our own prior work [7] may be due to the similarity in equipment and use of the identical contraction level. In the end, various factors may influence the EMG PDF, including: electrode shape, size and inter-electrode distance; contraction level; and muscle studied.

EMGσ Estimates

Our root mean square error results from the amplitude-modulated ramp contractions show that noise correction is most important at the lowest contractions levels. RDS processing has the advantage of being progressively less noticeable as effort level increases. For example, once the true EMGσ is four times that of the noise standard deviation, the RDS adjustment is only one sixteenth of the true EMGσ. Once the true EMGσ is five times the noise standard deviation, RDS adjustment is only one 25th the true EMGσ. Etc.

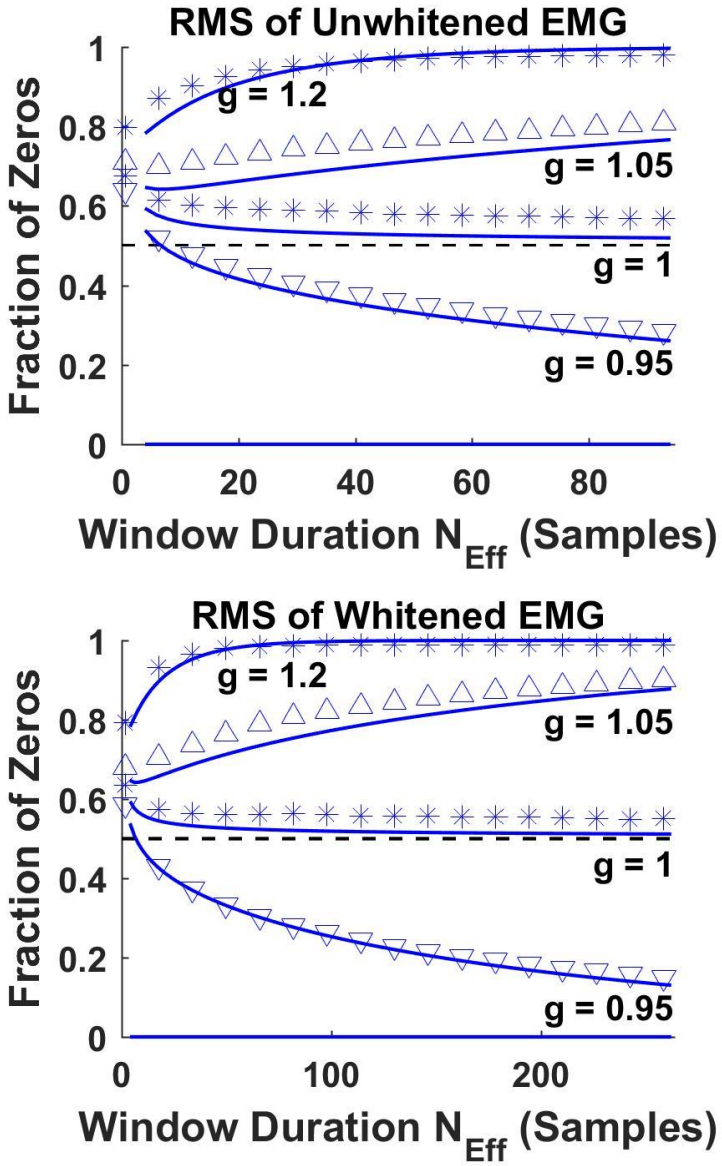

Fig. 4. Symbols show fraction of EMGσ values equal to zero during rest contractions for unwhitened (top) and whitened (bottom) experimental moving average RMS estimates as a function of effective number of samples NEff, for four different noise gain values "g". Solid lines show corresponding theoretic probabilities of zero values (same as Fig. 1), for comparison. Dash line show 0.5 probability.

Estimator Performance During Rest

For the ML estimate (c.f., g = 1 in Fig. 1 and Fig. 4), we have shown that approximately 50% of EMGσ estimates will be zero, based on either the Gaussian or

Laplacian model (excluding unrealistically small *NEff* values). Accordingly, nearly half of all EMGσ estimates will be greater than zero during rest! In some applications, this result is problematic. For example, the pose of myoelectrically-controlled prostheses, orthoses and exoskeletons would slowly drift at rest, producing an undesired and potentially dangerous action. Thus, we suggest that undesired non-zero EMGσ estimates during rest be eliminated by accentuating the noise standard deviation (i.e., setting g > 1). Fig. 1 shows that even modest increases in the gain factor g result in much lower probability of a non-zero value. Indeed, it is common to include threshold subtraction in a prosthesis EMG processor (with zero as the boundary condition), although it is currently applied by subtracting the noise standard deviation from EMG RMS (or MAV) and not via RDS processing [61, 62].

Note that many biomechanics studies in which the subject is active most of the time might not want to increase the gain factor "g". Doing so might create a bias in EMGσ-force estimates.

Limitations

Our theoretical models assumed independent samples, which are approximated in experimental analysis via whitening. However, since signal and noise have some distinctions in their spectral shape (noise exhibits a lower span of power across frequency [3]), one filter cannot precisely whiten both the noise-free EMG signal and the noise. In particular, whitening filters calibrated to active EMG may contain excessive high frequency gain [45]. Thus, some signal correlation will remain. This dissonance may place practical limits on the bandwidth of whitening filters [50], and might argue for the use of RDS processing in concert with other noise mitigation techniques such as adaptive whitening [3] —in which an adaptive Wiener filter provides lowpass filtering with a progressively lower cutoff at lower EMGσ levels.

When evaluating the fraction of zero EMGσ values during a rest contraction, we used that same rest contraction to estimate the noise variance (q^2). In practice, q^2 may vary over time; thus, so would the fraction of zero EMGσ values during rest. Hence, setting the noise gain factor "g" above one might help to mitigate unmeasured changes

in q^2.

V. CONCLUSION

Using established stochastic models for EMG in the presence of additive noise, we derived that RDS processing represents the ML estimate of EMGσ, under both Gaussian and Laplacian PDF assumptions. We concomitantly showed that EMGσ should be set to zero whenever RDS processing produces a negative-valued result. Further, we showed that the ML estimate at rest produces zero EMGσ estimates only 50% of the time (for all but short-duration smoothing windows). Experimentally, our biceps-triceps EMG data more closely followed a Gaussian PDF than a Laplacian PDF. Our EMGσ estimates closely followed theoretical predictions, both during ramp and rest contractions. This work definitively argues that EMG processors should use RDS processing rather than subtracting the noise standard deviation from EMG RMS (or MAV).

REFERENCES FOR THIS CHAPTER

[1] E. Kaiser and I. Petersen, "Adaptive Filter for EMG Control Signals," in *The Control of Upper-Extremity Prostheses and Orthoses*, P. Herberts, R. Kadefors, R. Magnusson, and I. Petersen, Eds., Springfield, IL: Charles C. Thomas, 1974, pp. 54–57.

[2] N. Hogan and R. W. Mann, "Myoelectric signal processing: Optimal estimation applied to electromyography—Part I: Derivation of the optimal myoprocessor," *IEEE Trans. Biomed. Eng.*, vol. 27, no. 7, pp. 382–395, 1980.

[3] E. A. Clancy and K. A. Farry, "Adaptive whitening of the electromyogram to improve amplitude estimation," *IEEE Trans. Biomed. Eng.*, vol. 47, no. 6, pp. 709–719, 2000.

[4] N. Hogan and R. W. Mann, "Myoelectric signal processing: Optimal estimation applied to electromyography—Part II: Experimental demonstration of optimal myoprocessor performance," *IEEE Trans. Biomed. Eng.*, vol. 27, no. 7, pp. 396–410, 1980.

[5] E. A. Clancy and N. Hogan, "Single site electromyograph amplitude estimation," *IEEE Trans. Biomed. Eng.*, vol. 41, no. 2, pp. 159–167, 1994.

[6] E. A. Clancy and N. Hogan, "Multiple site electromyograph amplitude estimation," *IEEE Trans. Biomed. Eng.*, vol. 42, no. 2, pp. 203–211, 1995.

[7] E. A. Clancy and N. Hogan, "Probability density of the surface electromyogram and its relation to amplitude detectors," *IEEE Trans. Biomed. Eng.*, vol. 46, no. 6, pp. 730–739, 1999.

[8] C. Dai, B. Bardizbanian, and E. A. Clancy, "Comparison of constant-posture force-varying EMG-force dynamic models about the elbow," *IEEE Trans. Neural Sys. Rehabil. Eng.*, no. 9, pp. 1529–1538, 2017.

[9] C. Dai, Z. Zhu, C. Martinez-Luna, T. R. Hunt, T. R. Farrell, and E. A. Clancy, "Two degrees of freedom, dynamic, hand-wrist EMG-force using a minimum number of electrodes," *J. Electromyo. Kinesiol.,* vol. 47, pp. 10–18, 2019.

[10] D. Staudenmann, K. Roeleveld, D. F. Stegeman, and J. H. van Dieen, "Methodological aspects of EMG recordings for force estimation—A tutorial and review," *J Electromyogr Kinesiol,* vol. 20, pp. 375–387, 2010.

[11] J. Hashemi, E. Morin, P. Mousavi, K. Mountjoy, and K. Hashtrudi-Zaad, "EMG-force modeling using parallel cascade identification," *J Electromyogr Kinesiol,* vol. 22, pp. 469–477, 2012.

[12] J. Hashemi, E. Morin, P. Mousavi, and K. Hashtrudi-Zaad, "Enhanced dynamic EMG-force estimation through calibration and PCI modeling," *IEEE Trans. Neural Sys. Rehabil. Eng.,* vol. 23, no. 1, pp. 41–50, 2015.

[13] E. P. Doheny, M. M. Lowery, D. P. FitzPatrick, and M. J. O'Malley, "Effect of elbow joint angle on force-EMG relationships in human elbow flexor and extensor muscles," *J Electromyogr Kinesiol,* vol. 18, pp. 760–770, 2008.

[14] C. Dai, S. Martel, F. Martel, D. Rancourt, and E. A. Clancy, "Single-trial estimation of quasi-static EMG-to-joint-mechanical-impedance relationship over a range of joint torques," *J. Electromyo. Kinesiol.,* vol. 45, pp. 18–25, 2019.

[15] C. J. Abul-Haj and N. Hogan, "Functional assessment of control systems for cybernetic elbow prosthesis—Part I: Description of the technique," *IEEE Trans. Biomed. Eng.,* vol. 37, no. 11, pp. 1025–1036, 1990.

[16] D. Shin, J. Kim, and Y. Koike, "A myokinetic arm model for estimating joint torque and stiffness from EMG signals during maintained posture," *J. Neurophysiol.,* vol. 101, pp. 387–401, 2009.

[17] T. Kawase, H. Kambara, and Y. Koike, "A power assist device based on joint equilibrium point estimation from EMG signals," *J. Robot. Mechatron.,* vol. 24, no. 1, pp. 205–218, 2012.

[18] S. Pfeifer, H. Vallery, M. Hardegger, R. Riener, and E. J. Perreault, "Model-based estimation of knee stiffness," *IEEE Trans. Biomed. Eng.,* vol. 59, no. 9, pp. 2604–2612, 2012.

[19] M. A. Golkar, E. S. Tehrani, and R. E. Kearney, "Linear parametric varying identification of dynamic joint stiffness during time-varying voluntary contractions," *Front. Comput. Neurosci.,* vol. 11, p. 35, 2017.

[20] D. J. Ostry and A. G. Feldman, "A critical evaluation of the force control hypothesis in motor control," *Exp. Brain Res.,* vol. 153, pp. 275–288, 2003.

[21] P. Parker, K. Englehart, and B. Hudgins, "Myoelectric signal processing for control of powered limb prostheses," *J. Electromyo. Kinesiol.,* vol. 16, pp. 541–548, 2006.

[22] D. Farina *et al.,* "The extraction of neural information from the surface EMG for the control of upper-limb prostheses: Emerging avenues and Challenges," *IEEE Trans. Neural Sys. Rehabil. Eng.,* vol. 22, no. 4, pp. 797–809, 2014.

[23] R. A. Popat *et al.,* "Quantitative assessment of four men using above-elbow prosthetic control," *Arch. Phys. Med. Rehabil.,* vol. 74, pp. 720–729, 1993.

[24] G. M. Hagg, B. Melin, and R. Kadefors, "Applications in ergonomics," in *Electromyography: Physiology, Engineering, and Noninvasive Applications*, R. Merletti and P. A. Parker, Eds.: IEEE Press/Wiley-Interscience, 2004, pp. 343–363.

[25] S. Kumar and A. Mital, *Electromyography in Ergonomics*. Briston, PA: Taylor & Francis, 1996.

[26] C. Disselhorst-Klug, T. Schmitz-Rode, and G. Rau, "Surface electromyography and muscle force: Limits in sEMG-force relationship and new approaches for applications," *Clin. Biomech.*, vol. 24, pp. 225–235, 2009.

[27] C. A. M. Doorenbosch and J. Harlaar, "A clinically applicable EMG-force model to quantify active stabilization of the knee after a lesion of the anterior cruciate ligament," *Clin. Biomech.*, vol. 18, pp. 142–149, 2003.

[28] R. Merletti, A. Botter, and U. Barone, "Detection and conditioning of surface EMG signals," in *Surface Electromyography; Physiology, Engineering, and Applications*, R. Merlett and D. Farina, Eds., Hoboken, New Jersey: John Wiley & Sons, Inc., 2016, pp. 54–90.

[29] E. A. Clancy, E. L. Morin, and R. Merletti, "Sampling, noise-reduction and amplitude estimation issues in surface electromyography," *J. Electromyo. Kinesiol.*, vol. 12, pp. 1–16, 2002.

[30] E. A. Clancy, "Electromyogram amplitude estimation with adaptive smoothing window length," *IEEE Trans. Biomed. Eng.*, vol. 46, no. 6, pp. 717–729, 1999.

[31] E. A. Clancy, D. Farina, and R. Merletti, "Cross-comparison of time- and frequency-domain methods for monitoring the myoelectric signal during a cyclic, force-varying, fatiguing hand-grip task," *J. Electromyo. Kinesiol.*, vol. 15, pp. 256–265, 2005.

[32] P. Liu, L. Liu, F. Martel, D. Rancourt, and E. A. Clancy, "Influence of joint angle on EMG-torque model during constant-posture quasi-constant-torque contractions," *J. Electromyo. Kinesiol.*, vol. 23, pp. 1020–1028, 2013.

[33] P. Liu, L. Liu, and E. A. Clancy, "Influence of joint angle on EMG-torque model during constant-posture, torque-varying contractions," *IEEE Trans. Neural Sys. Rehabil. Eng.*, vol. 23, no. 6, pp. 1039–1046, 2015.

[34] E. A. Clancy, C. Martinez-Luna, M. Wartenberg, C. Dai, and T. Farrell, "Two degrees of freedom quasi-static EMG-force at the wrist using a minimum number of electrodes," *J Electromyogr Kinesiol*, vol. 34, pp. 24–36, 2017.

[35] P. A. Parker, J. A. Stuller, and R. N. Scott, "Signal processing for the multistate myoelectric channel," *Proc. IEEE*, vol. 65, no. 5, pp. 662–674, 1977.

[36] Y. T. Zhang, P. A. Parker, and R. N. Scott, "Control performance characteristics of myelectric signal with additive interference," *Med. Biol. Eng. Comput.*, vol. 29, pp. 84–88, 1991.

[37] P. A. Parker and R. N. Scott, "Myoelectric control of prostheses," *CRC Crit. Reviews Biomed. Eng.*, vol. 13, no. 4, pp. 283–310, 1986.

[38] P. Bonato, T. D'Alessio, and M. Knaflitz, "A statistical method for the measurement of muscle activation intervals from surface myoelectric signal during gait," *IEEE Trans. Biomed. Eng.*, vol. 45, no. 3, pp. 287–299, 1998.

[39] R. V. Baratta, M. Solomonow, and B.-H. Zhu, "Methods to reduce the variability of EMG power spectrum estimates," *J. Electromyo. Kinesiol.*, vol. 8, pp. 279–285, 1998.

[40] K. Koirala, M. Dasog, P. Liu, and E. A. Clancy, "Using the electromyogram to anticipate torques about the elbow," *IEEE Trans. Neural Sys. Rehabil. Eng.*, vol. 23, no. 3, pp. 396–402, 2015.

[41] L. Frey Law, C. Krishnan, and K. Avin, "Modeling nonlinear errors in surface electromyography due to baseline noise: A new methodology," *J. Biomech.*, vol. 44, pp. 202–205, 2011.

[42] R. Ortengren, "Noise and artefacts," in *Electromyography in Ergonomics*, S. Kumar and A. Mital, Eds., London: Taylor & Francis, 1996, pp. 97–107.

[43] G.-A. Hansson, "Letter to the editor," *J. Biomech.*, vol. 44, p. 1637, 2011.

[44] L. Frey Law, K. Avin, and C. Krishnan, "Response to letter to the editor," *J. Biomech.*, vol. 44, pp. 1637–1638, 2011.

[45] E. A. Clancy, "Stochastic Modeling of the Relationship Between the Surface Electromygram and Muscle Torque," Ph.D Thesis, Massachusetts Institute of Technology, p. 303–352, 449–469, 1991.

[46] E. A. Clancy, in *Optimal Electromyogram Modeling and Processing During Active Contractions and Rest*: Haopeng Wang M.S. Thesis, Worcester Polytechnic Institute, 2019, pp. 40–58.

[47] G. B. Thomas Jr., M. D. Weir, J. Hass, and C. Heil, in *Thomas' Calculus*13th ed., Boston, MA: Pearson, 2014, pp. 185–193.

[48] A. W. Drake, in *Fundamentals of Applied Probability Theory*, New York: McGraw-Hill Book Company, 1967, pp. 103–107, 273–274.

[49] P. Prakash, C. A. Salini, J. A. Tranquilli, D. R. Brown, and E. A. Clancy, "Adaptive whitening in electromyogram amplitude estimation for epoch-based applications," *IEEE Trans. Biomed. Eng.*, vol. 52, no. 2, pp. 331–334, 2005.

[50] M. Dasog, K. Koirala, P. Liu, and E. A. Clancy, "Electromyogram bandwidth requirements when the signal is whitened," *IEEE Trans. Neural Sys. Rehabil. Eng.*, vol. 22, no. 3, pp. 664–670, 2014.

[51] J. S. Bendat and A. G. Piersol, in *Random Data: Analysis and Measurement Procedures*, New York: John Wiley and Sons, Inc., 1971, pp. 277–281.

[52] L. Liu, P. Liu, E. A. Clancy, E. Scheme, and K. B. Englehart, "Electromyogram whitening for improved classification accuracy in upper limb prosthesis control," *IEEE Trans. Neural Sys. Rehabil. Eng.*, vol. 21, no. 5, pp. 767–774, 2013.

[53] R. B. Jerard, T. W. Williams, and C. W. Ohlenbusch, "Practical design of an EMG controlled above elbow prosthesis," in *Proc. 1974 Conf. Eng. Devices Rehabil.*, Boston, MA, 1974, pp. 73–77.

[54] T. D'Alessio, "Analysis of a digital EMG signal processor in dynamic conditions," *IEEE Trans. Biomed. Eng.*, vol. 32, pp. 78–82, 1985.

[55] E. Park and S. G. Meek, "Adaptive filter of the electromyographic signal for prosthetic control and force estimation," *IEEE Trans. Biomed. Eng.*, vol. 42, pp. 1048–1052, 1995.

[56] S. Ranaldi, C. De Marchis, and S. Conforto, "An automatic, adaptive, information-based algorithm for the extraction of the sEMG envelope," *J. Electromyo. Kinesiol.*, vol. 42, pp. 1–9, 2018.

[57] H. Roesler, "Statistical analysis and evaluation of myoelectric signals for proportional control," in *The Control of Upper-Extremity Prosthesis and Orthoses*, Springfield, IL: Thomas, 1974, pp. 44–53.

[58] I. W. Hunter, R. E. Kearney, and L. A. Jones, "Estimation of the conduction velocity of muscle action potentials using phase and impulse response function techniques," *Med. Biol. Eng. Comput.*, vol. 25, pp. 121–126, 1987.

[59] M. Bilodeau, M. Cincera, A. B. Arsenault, and D. Gravel, "Normality and stationarity of EMG signals of elbow flexor muscles during ramp and step isometric contractions," *J. Electromyo. Kinesiol.*, vol. 7, no. 2, pp. 87–96, 1997.

[60] K. Nazarpour, A. Al-Timemy, G. Bugmann, and A. Jackson, "A note on the probability distrubution function of the surface electromyogram signal," *Brain Res. Bull.*, vol. 90, pp. 88–91, 2013.

[61] T. W. Williams III, "Practical methods for controlling powered upper-extremity prostheses," *Assist. Technol.*, vol. 2, pp. 3–18, 1990.

[62] J. M. Hahne, M. A. Schweisfurth, M. Koppe, and D. Farina, "Simultaneous control of multiple functions of bionic hand prostheses: Performance and robustness in end users," *Sci. Robot.*, vol. 3, p. eaat3630, 2018.

CONCLUSION

By using the ensemble-averaged 512 subject-specific whitening filter shape and normalized average noise signal spectrum, a 60th-order "Universal" FIR whitening filter was calibrated. Compared to the original subject-specific whitening filter, the performance of this universal filter had no significant difference in a statistical test. However, since the whitening shape and noise input are fixed, calibration time can be saved, which is much more convenient and simpler.

The whitening filter is very close in shape to a highpass filter. Potvin [1] found that a low-order, fixed IIR highpass filter was implemented to function as a whitening filter. Thus, to further simplify the "Universal" FIR whitening filter, a 2nd-order "Universal" IIR whitening filter was designed by using a differential evolution algorithm and the universal whitening shape as the input of the cost function. The performance of this IIR filter is very similar to the FIR whitening filter. However, with much less coefficients, this IIR filter is even more convenient to implement. Thus, we simplified the 60th-order subject-specific FIR whitening filter method, which is very time consuming, to a 2nd-order IIR whitening filter.

Under both Gaussian and Laplacian PDF assumptions, root-difference-square (RDS) processing was shown to be optimal (in the maximum likelihood sense) for estimating EMGσ from the EMG signal with additive noise. Also, it was proven that our biceps-triceps EMG signal more closely followed a Gaussian PDF. Results from our "ramp" test and 0% MVC (rest) trials indicates that EMG processors should use RDS instead of subtracting the noise standard deviation from EMG RMS or MAV. This RDS processor was implemented with different whitening methods. Results show that with a proper whitening band limit frequency (~600 Hz), there is barely no loss of performance compared to methods without RDS. We showed that the influence of RDS processing is limited in high contraction levels, and it is necessary in low contraction levels.

References:

[1] Potvin et al. J Electromyo Kinesiol. 2004;14:389–399.

APPENDIX I

I. INTRODUCTION

This is the appendix for the submitted paper "*Optimal Estimation of EMG Standard Deviation (EMGσ) Requires Noise Subtraction in the Power Domain: Model-Based Derivations and their Implications*" (Chapter 3). This appendix will include details about methods, results that were not shown in the journal paper and all the necessary analysis and discussion of the results.

There are two basic parts in this appendix. The first part is about the "Ramp" test. Details about the method will be introduced, statistical test results will be shown in a table, all other results will be shown in figures. The second part is about testing the noise subtraction using "real" data (512 trials mentioned in the Chapter 2, 3 and 4). All the results will be shown in tables.

II. PART 1

EMG Ramp Study Methods

First, a 5 second "Ramp" was created. For this ramp: 0 in the first second, from 0 to 0.1 for 2-4 seconds, 0.1 in the last one second. Then all the 512 trials were processed in the following method:

- Highpass (4^{th} order, 15Hz);
- Notch filter for powerline interference and its harmonics;
- Process EMG by whitening/unwhitening (whitening band limit at 600 Hz);
- Normalize the standard deviation of both 50% and, separately, 0% MVC to 1;
- Modulate EMG by multiplying the signal by ramp and multiplying the noise by 0.02 and adding them together;
- Process EMG by MAV/RMS estimator (For the results, we only used RMS since it has a much better performance);
- Omit the first 0.25 seconds and the last 0.25 seconds;

- Noise subtraction or without noise subtraction;
- Compute the RMSE between the EMGσ and ramp;

Overall result

Here are the rms errors through 512 trials for all the tested methods. Without the adaptive noise canceller, whiten with noise subtraction is the best method we can use, whiten and unwhitened without noise subtraction have very similar performances. (RMS estimator)

TABLE 1.

AVERAGED RMSE FOR ALL 512 TRIALS USING RMS ESTIMATOR

Method	RMSE(mean±std)
Unwhiten	0.0122±0.0025
Unwhiten NS	0.0076±0.0031
Whiten	0.0121±0.0022
Whiten NS	0.0071±0.0030

For MAV estimator:

TABLE 2.

AVERAGED RMSE FOR ALL 512 TRIALS USING MAV ESTIMATOR

Method	RMSE(mean±std)
Unwhiten	0.0148±0.0021
Unwhiten NS	0.0161±0.0023
Whiten	0.0146±0.0020
Whiten NS	0.0158±0.0022

Statistical results

To achieve a more convincing conclusion, we used paired-sign test to get the statistical results (due to the non-normality of our data). The results below are the *p* values for each combination at each specific time within the ramp we chose (before Bonferroni correction).

TABLE 3.

STATISTICAL TEST RESULTS FOR EACH METHOD AT SELECTED TIMES USING PAIRED-SIGN TEST.

Time (s)	Wh/Wh+NS	Wh/Un	Wh/Un+NS	Wh+NS/Un	Wh+NS/Un+NS	Un/Un+NS
0.5	7.4583e-155	0.0095	6.2585e-128	7.4583e-155	1.6452e-31	7.4583e-155
1	7.4583e-155	0.2537	3.8261e-152	7.4583e-155	3.0624e-28	7.4583e-155
1.5	7.8943e-118	1.2771e-05	2.7108e-98	7.6992e-114	9.8245e-10	6.1165e-84
2	1.4433e-36	0.0510	1.7448e-32	1.7448e-32	0.0095	8.6218e-28
2.5	3.1902e-10	0.0286	2.6690e-07	6.6618e-07	0.0035	1.0400e-06

3	0.0151	0.3454	0.0286	0.1346	0.0286	0.0286
3.5	0.1547	0.0188	0.3454	0.5176	0.0151	0.2263
4	0.4824	0.1547	0.0609	0.4824	0.1767	0.2537
4.5	2.3460e-04	0.0723	0.0853	0.0075	0.0233	0.0027

Other results

Comparing Ramp with EMGσ along time.

For RMS estimator:

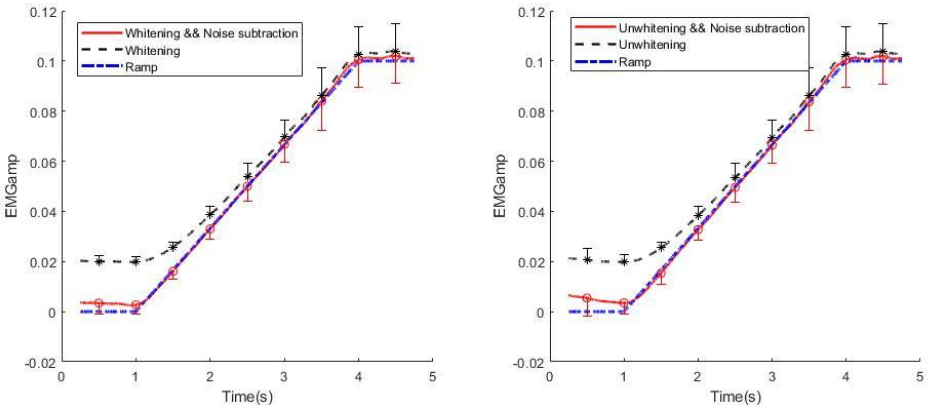

Fig. 1. Left shows ensemble averaged whitened EMGσ (using RMS estimator) with or without noise subtraction along the "Ramp", symbols and error bars show mean and std at times: 0.5, 1, 1.5…..4.5. Right shows Unwhitened method results.

For MAV estimator:

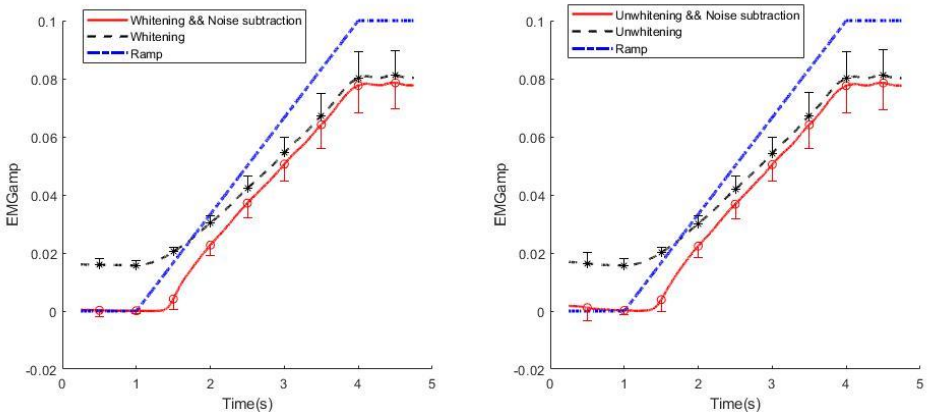

Fig. 2. Left shows ensemble averaged whitened EMGσ (using MAV estimator) with or without noise subtraction along the "Ramp", symbols and error bars show mean and std at times: 0.5, 1, 1.5…..4.5. Right shows Unwhitened method results.

For all possible methods, also computed the RMSE between ramp and EMGσ processed along the time (the figure is error vs time). Here, we only used the subject-specific adaptive whitening filter to compare with unwhitened method.

RMS estimator:

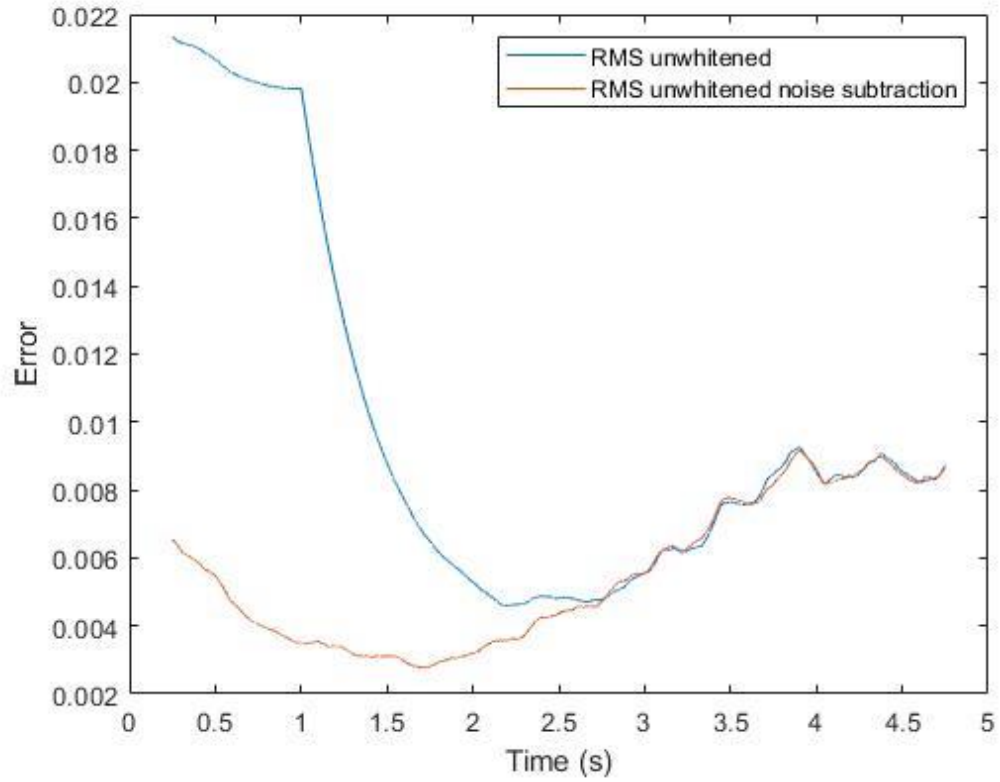

Fig. 3. Error comparison (along time) between unwhiten without noise subtraction and unwhiten with noise subtraction using RMS estimator.

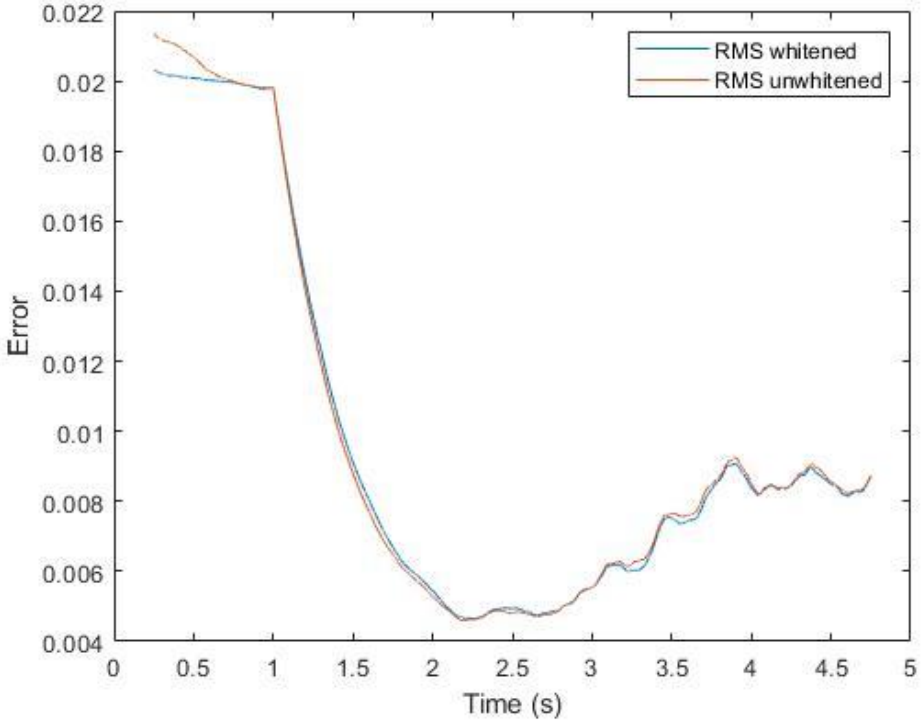

Fig. 4. Error comparison between whiten and unwhiten both without noise subtraction using RMS estimator.

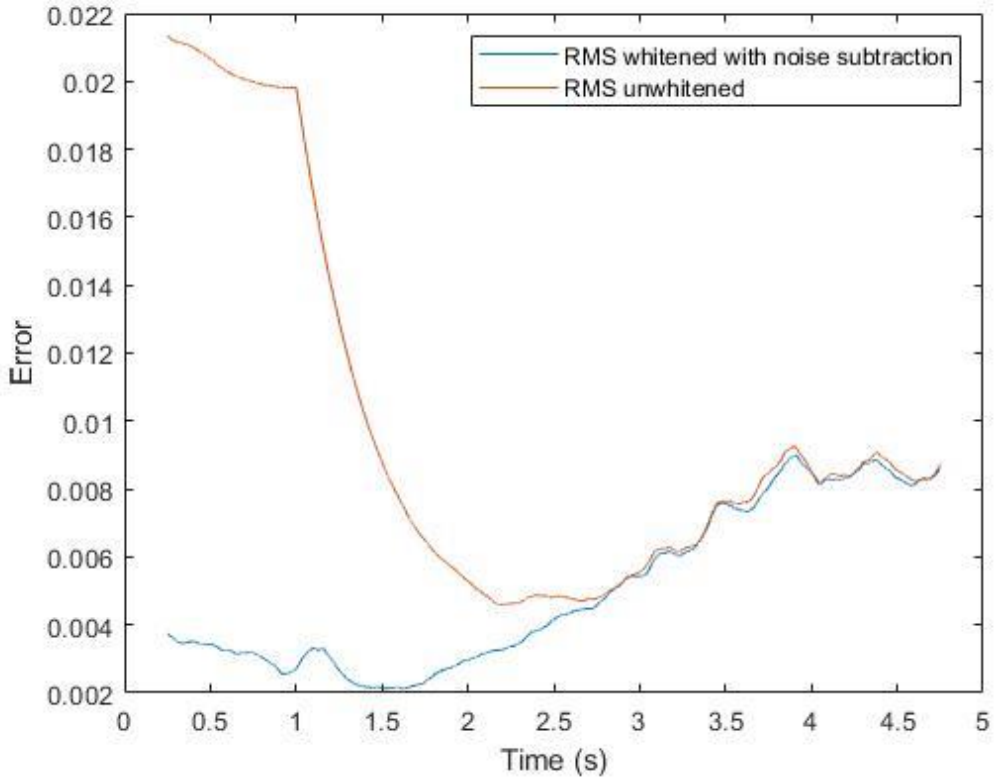

Fig. 5. Error comparison (along time) between whiten with noise subtraction and unwhiten without noise subtraction using RMS estimator.

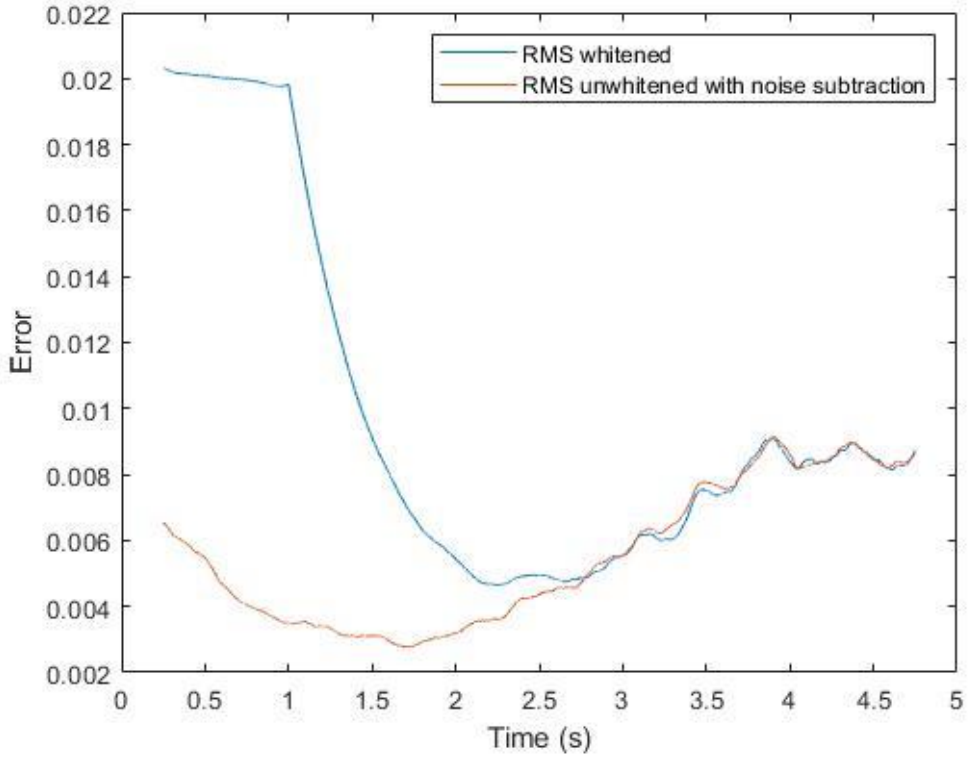

Fig. 6. Error comparison (along time) between whiten without noise subtraction and unwhiten with noise subtraction using RMS estimator.

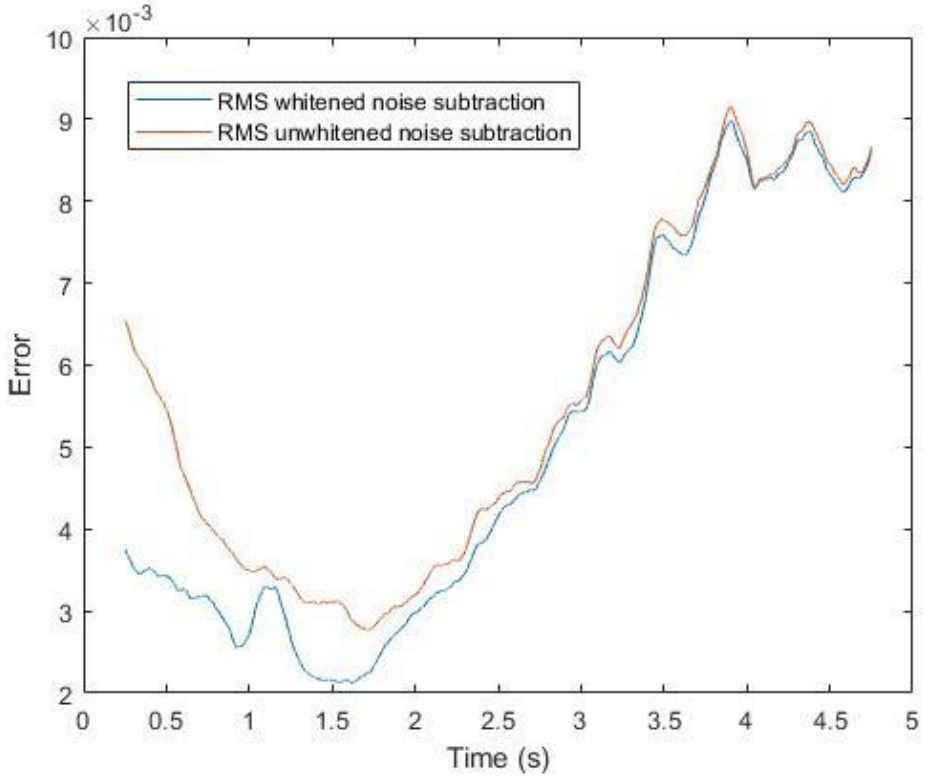

Fig. 7. Error comparison (along time) between whiten with noise subtraction and unwhiten with noise subtraction using RMS estimator.

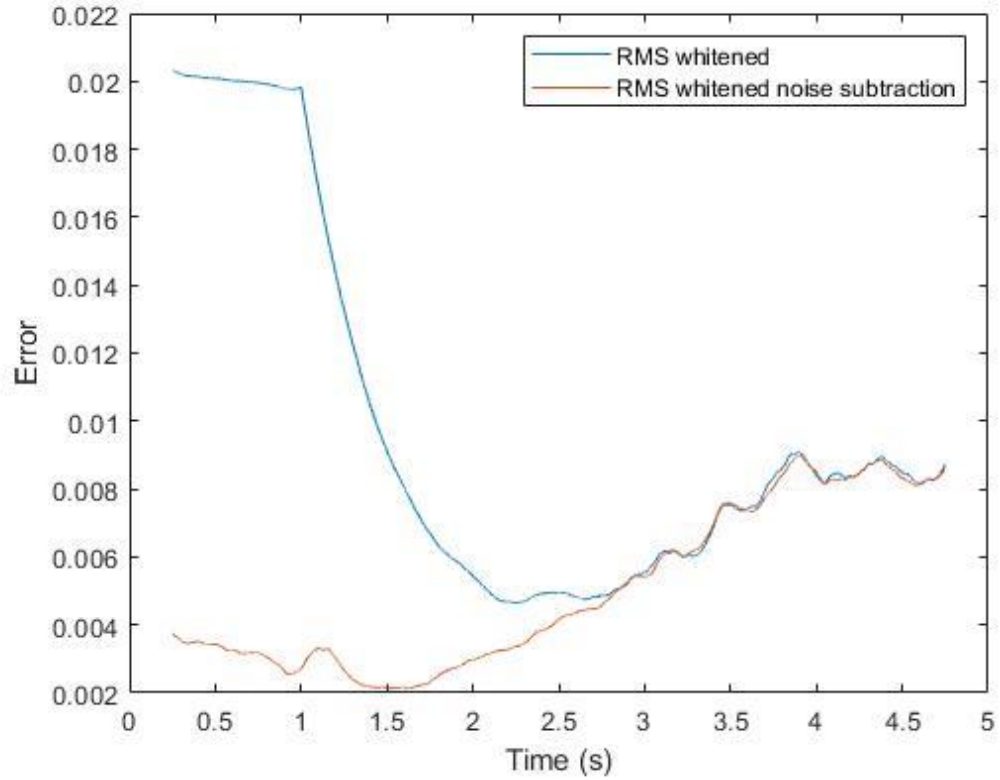

Fig. 8. Error comparison (along time) between whiten without noise subtraction and whiten using noise subtraction using RMS estimator.

MAV estimator:

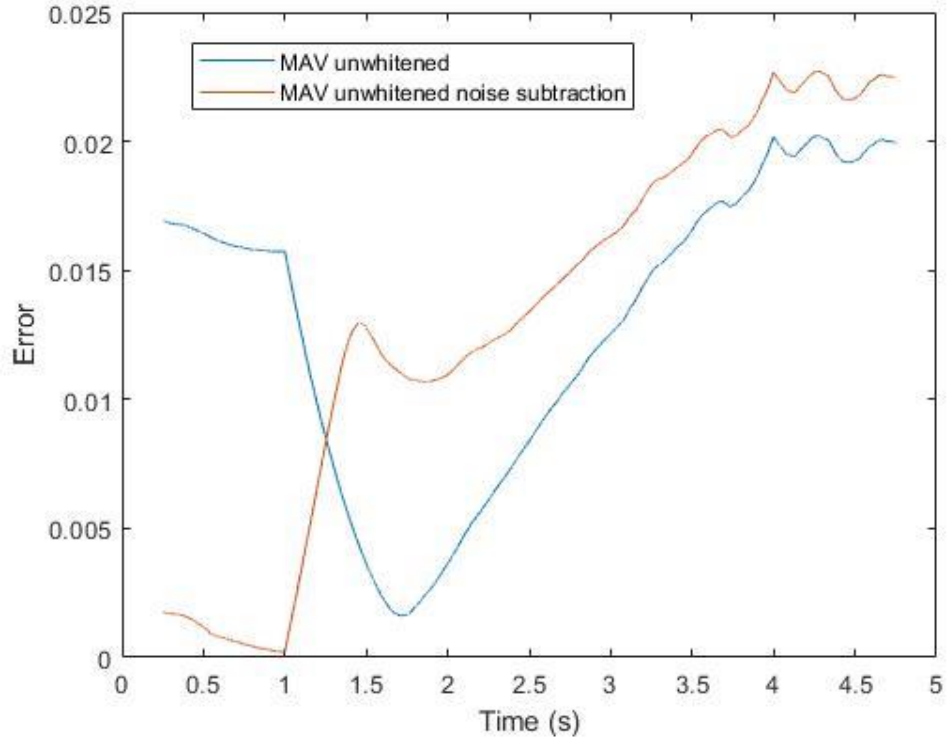

Fig. 9. Error comparison (along time) between unwhiten without noise subtraction and unwhiten with noise subtraction using MAV estimator.

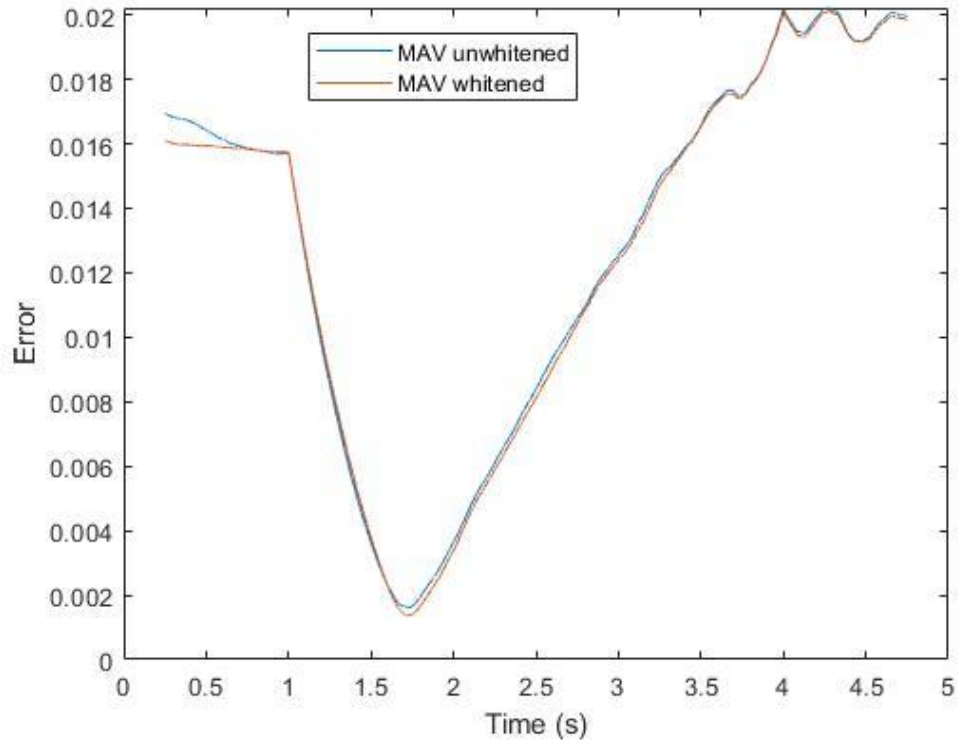

Fig. 10. Error comparison between whiten and unwhiten both without noise subtraction using MAV estimator.

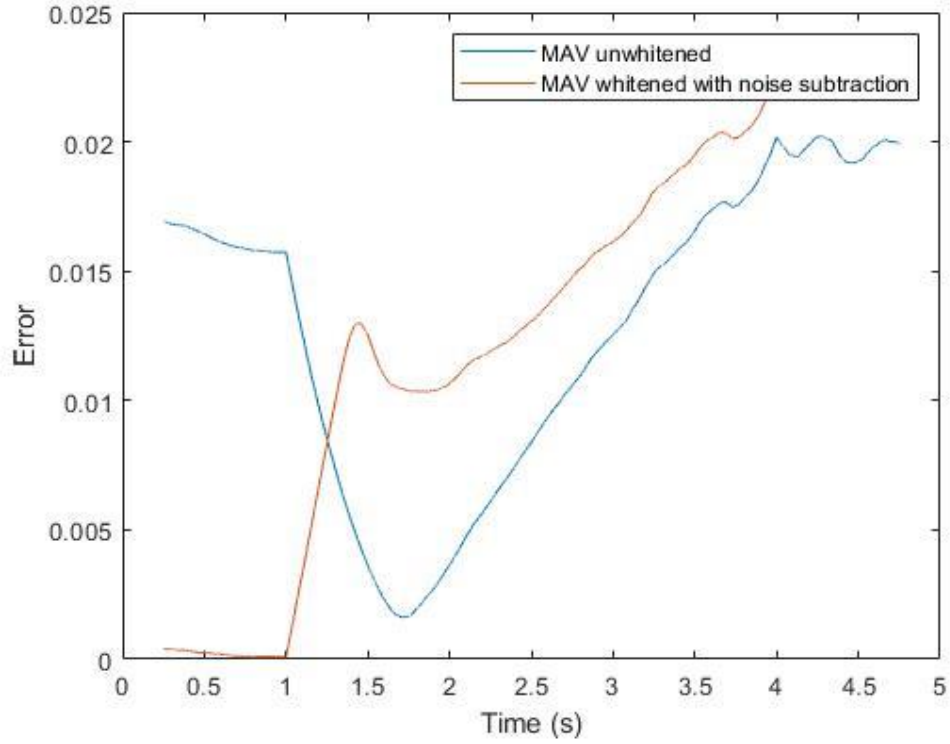

Fig. 11. Error comparison (along time) between whiten with noise subtraction and unwhiten without noise subtraction using MAV estimator.

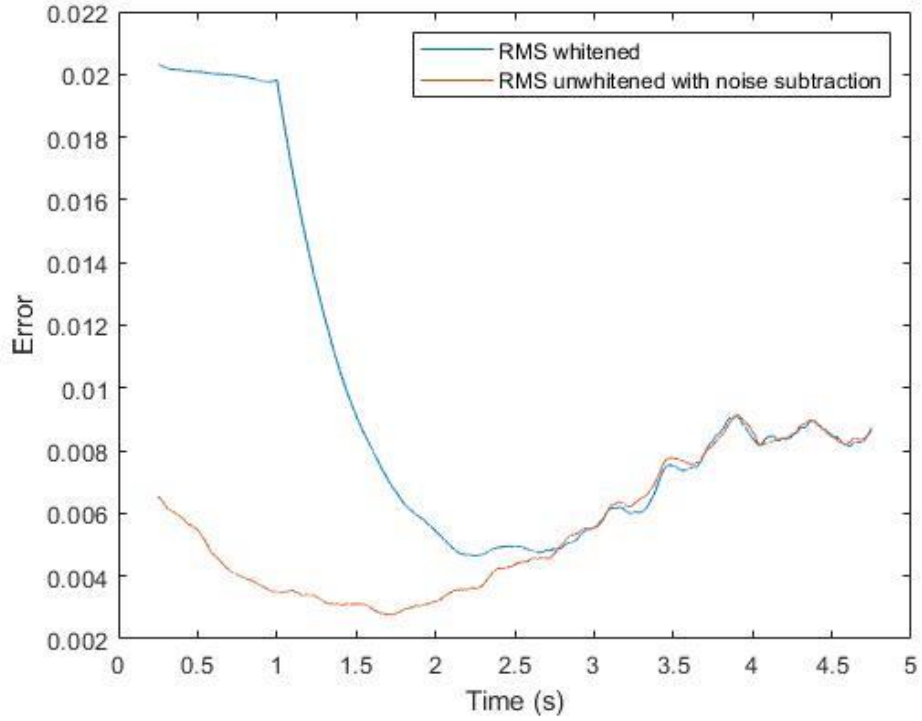

Fig. 12. Error comparison (along time) between whiten without noise subtraction and unwhiten with noise subtraction using MAV estimator.

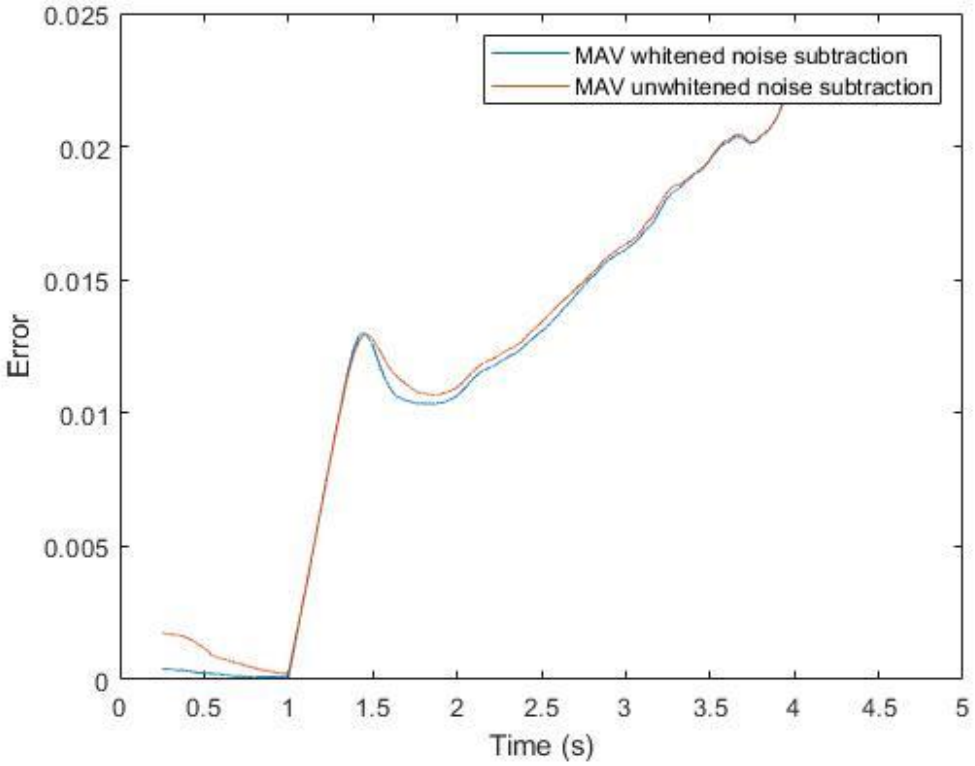

Fig. 13. Error comparison (along time) between whiten with noise subtraction and unwhiten with noise subtraction using MAV estimator.

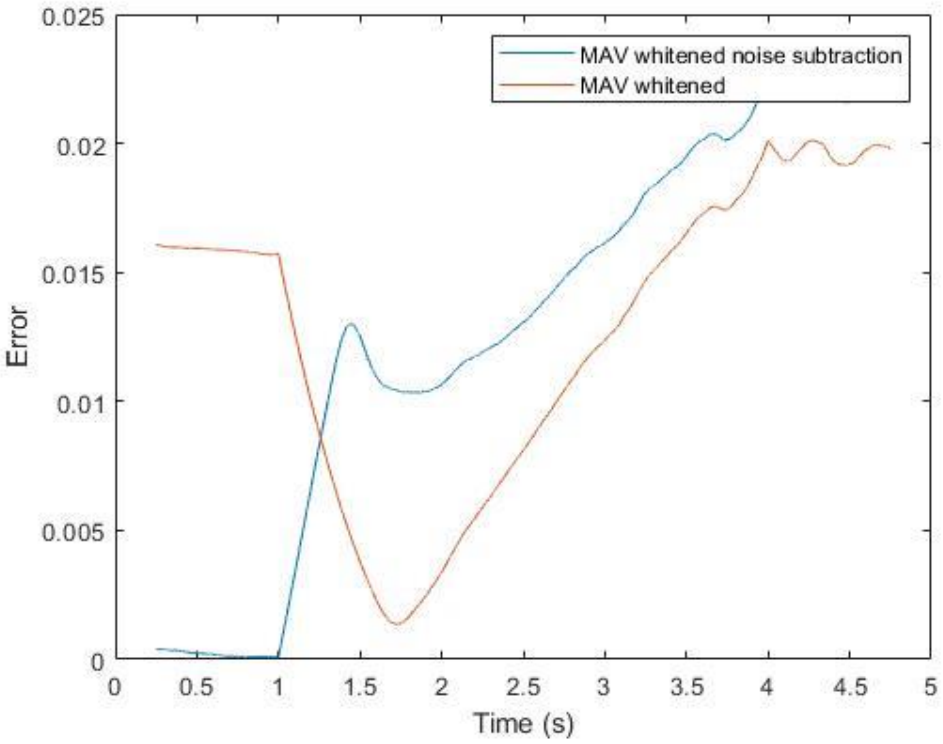

Fig. 14. Error comparison (along time) between whiten without noise subtraction and whiten using noise subtraction using MAV estimator.

III. PART 2

Tables below show the results tested by using 512 trials collected previously. The results are RMSE between the real torque and the estimated torque by using different EMG processing methods.

In order to remove the second stage of whitening filter, *Svv* was set to "0" (see details in the EMG Amplitude Estimation Toolbox).

The band limit frequency for whitening filter is varied from 200Hz to 1600Hz to see how it will affect the performances of different methods.

TABLE IV

THE PERFORMANCES OF DIFFERENT METHODS BY USING DIFFERENT WHITENING BAND LIMIT FREQUENCY.

Whitening band limit (Hz)	Method	RMSE (mean±std)
200	Original Whitened, RDS	5.55%±2.49%
	Original Whitened, Svv = 0	5.50%±2.40%
	Original Whitened, Svv = 0, RDS	5.56%±2.43%
	Universal FIR Whitened stage1 only, RDS	5.42%±2.34%
	Universal FIR whitened, stage1+average noise, RDS	5.38%±2.38%
	Universal FIR whitened with stage 1, Svv = 0	5.39%±2.45%
400	Original Whitened, RDS	5.05%±2.13%
	Original Whitened, Svv = 0	5.10%±2.27%
	Original Whitened, Svv = 0, RDS	5.11%±2.26%
	Universal FIR Whitened stage1 only, RDS	4.94%±1.95%
	Universal FIR whitened, stage1+average noise, RDS	4.92%±2.07%
	Universal FIR whitened with stage 1, Svv = 0	4.93%±2.13%
500	Original Whitened, RDS	4.95%±2.01%
	Original Whitened, Svv = 0	5.00%±2.16%
	Original Whitened, Svv = 0, RDS	5.04%±2.14%
	Universal FIR Whitened stage1 only, RDS	4.89%±1.96%
	Universal FIR whitened, stage1+average noise, RDS	4.86%±2.03%

	Universal FIR whitened with stage 1, Svv = 0	4.89%±2.14%
600	Original Whitened, RDS	4.85%±1.97%
	Original Whitened, Svv = 0	4.87%±2.11%
	Original Whitened, Svv = 0, RDS	4.96%±2.21%
	Universal FIR Whitened stage1 only, RDS	4.81%±1.99%
	Universal FIR whitened, stage1+average noise, RDS	4.80%±2.04%
	Universal FIR whitened with stage 1, Svv = 0	4.82%±2.15%
700	Original Whitened, RDS	4.83%±2.03%
	Original Whitened, Svv = 0	4.91%±2.13%
	Original Whitened, Svv = 0, RDS	4.94%±2.15%
	Universal FIR Whitened stage1 only, RDS	4.81%±2.00%
	Universal FIR whitened, stage1+average noise, RDS	4.81%±2.08%
	Universal FIR whitened with stage 1, Svv = 0	4.85%±2.24%
800	Original Whitened, RDS	4.80%±2.02%
	Original Whitened, Svv = 0	4.88%±2.06%
	Original Whitened, Svv = 0, RDS	4.95%±2.05%
	Universal FIR Whitened stage1 only, RDS	4.79%±2.04%
	Universal FIR whitened, stage1+average noise, RDS	4.79%±2.09%
	Universal FIR whitened with stage 1, Svv = 0	4.85%±2.23%
1000	Original Whitened, RDS	4.77%±2.07%
	Original Whitened, Svv = 0	4.93%±2.19%
	Original Whitened, Svv = 0, RDS	5.04%±2.09%
	Universal FIR Whitened stage1 only, RDS	4.75%±2.04%
	Universal FIR whitened, stage1+average noise, RDS	4.79%±2.09%
	Universal FIR whitened with stage 1, Svv = 0	4.85%±2.33%
	Original Whitened, RDS	4.76%±2.09%

1200	Original Whitened, Svv = 0	5.00%±2.20%
	Original Whitened, Svv = 0, RDS	5.27%±2.21%
	Universal FIR Whitened stage1 only, RDS	4.76%±2.06%
	Universal FIR whitened, stage1+average noise, RDS	4.74%±2.13%
	Universal FIR whitened with stage 1, Svv = 0	5.10%±2.37%
1400	Original Whitened, RDS	4.77%±2.12%
	Original Whitened, Svv = 0	5.19%±2.36%
	Original Whitened, Svv = 0, RDS	5.70%±2.65%
	Universal FIR Whitened stage1 only, RDS	4.76%±2.07%
	Universal FIR whitened, stage1+average noise, RDS	4.75%±2.11%
	Universal FIR whitened with stage 1, Svv = 0	5.35%±2.49%
1600	Original Whitened, RDS	4.77%±2.14%
	Original Whitened, Svv = 0	5.38%±2.46%
	Original Whitened, Svv = 0, RDS	6.00%±3.05%
	Universal FIR Whitened stage1 only, RDS	4.75%±2.06%
	Universal FIR whitened, stage1+average noise, RDS	4.74%±2.08%
	Universal FIR whitened with stage 1, Svv = 0	5.60%±2.52%

Using noise subtraction may lose some performances when removing the adaptive noise canceller (step 2 in adaptive whitening filter, Svv = 0). However, in certain range of whitening band frequencies, this loss of performance is acceptable since simplifying the adaptive whitening filter is also an important issue. For subject-specific whitening method with Svv = 0 and RDS processor, setting the whitening band frequency to 700Hz will achieve the optimal performance (4.94%±2.15%). For universal FIR whitening method (Svv = 0, NS), setting the whitening band frequency to 600Hz will achieve the optimal performance (4.90%±2.19%).

Results above also indicate that the original whitening method is very robust and reliable, the adaptive noise canceller always works well as the whitening band limit

varies.

Figures below show overall results tested above. Both methods achieve optimal performance when the whitening band limit at 600 ~ 700 Hz when using noise subtraction.

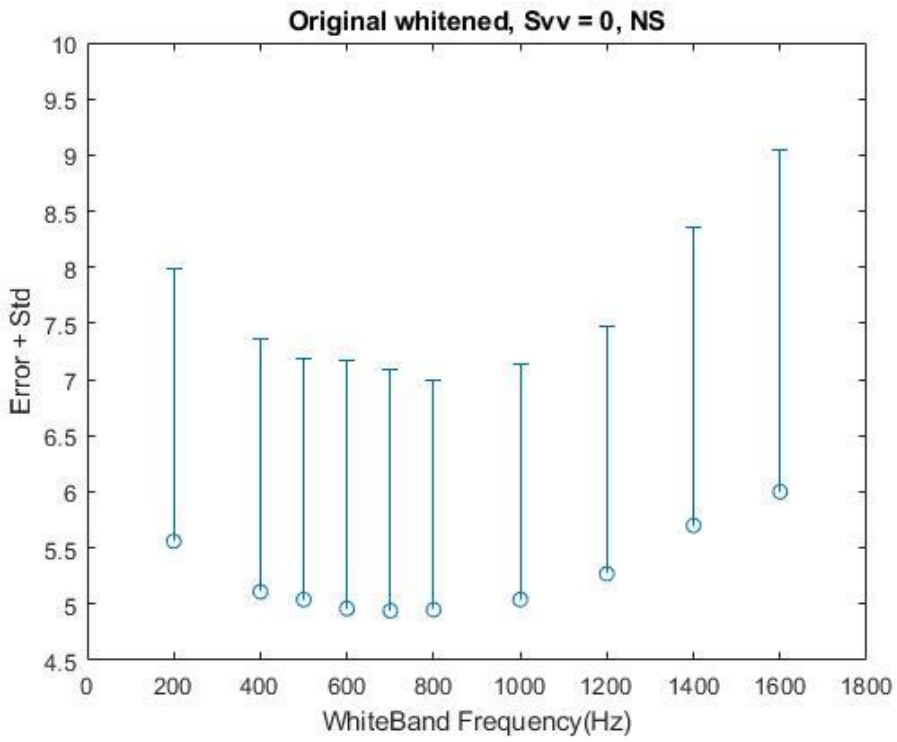

Fig. 15. The rms error + standard deviation between estimated force using original whitening method with noise subtraction and “real” torque along with different whitenband limit frequency.

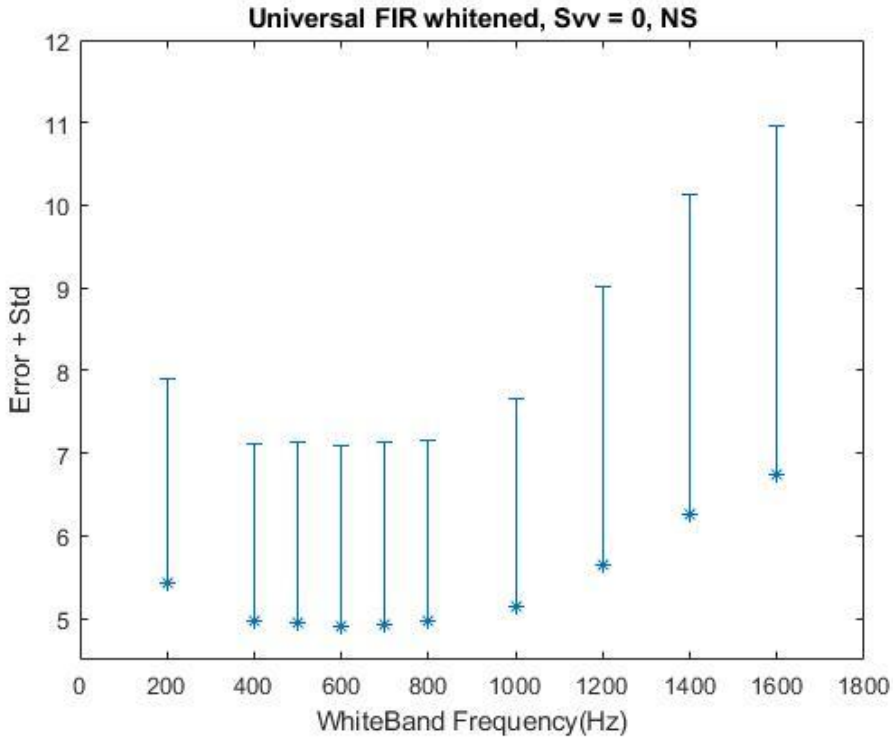

Fig. 16. The rms error + standard deviation between estimated force using universal whitening method with noise subtraction and “real” torque along with different whitenband limit frequency.

APPENDIX II DETAIL OF DATA USED IN THIS THESIS

Experiment 'LA'

'01'; '02'; '03'; '04'; '05'; '06'; '07'; '10'; '13'; '14'; '15'; '16'; '17'; '18'; '19'; '20'; '21';

Trial number for 0%MVC and 50% MVC extension and flexion

Trial '15' 0%MVC

Trial '10' 50% Extension

Trial '12' 50% Flexion

Subject 'LA18' trial '15' is a bad rest recording, this trial is substituted by trial '32' of subject 'LA18'

Experiment 'LB'

'02'; '03'; '05'; '07'; '08'; '09'; '10'; '12'; '13'; '16'; '17'; '18'; '19'; '20'; '21';

Trial number for 0%MVC and 50% MVC extension and flexion

Trial '15' 0%MVC

Trial '10' 50% Extension

Trial '12' 50% Flexion

Experiment 'wx'

'01'; '02'; '04'; '05'; '06'; '07'; '08'; '09'; '10'; '11'; '12'; '13'; '14'; '17'; '18'; '19'; '20'; '22'; '23'; '24'; '25'

Trial number for 0%MVC and 50% MVC extension and flexion

Trial '15' 0%MVC

Trial '10' 50% Extension

Trial '13' 50% Flexion

Experiment 'ww'

'01'; '02'; '03'; '04'; '05'; '06'; '08'; '09'; '10'; '11'; '12']

Trial number for 0%MVC and 50% MVC extension and flexion

Trial '15' 0%MVC

Trial '10' 50% Extension

Trial '12' 50% Flexion

Subject 'ww05' trial '15' is a bad rest recording, this trial is substituted by trial

‘39’ of subject ‘ww05’